Kinetics, Dynamics, Photochemistry, and Excited States UV Photochemistry of Acetylacetaldehyde Trapped in Cryogenic Matrices

Pierre Rousselot-Pailley, Sophie Sobanska, Nicolas Ferré, Stéphane Coussan

THE JOURNAL OF PHYSICAL CHEMISTRY A

A: Kinetics, Dynamics, Photochemistry, and Excited States

UV Photochemistry of Acetylacetaldehyde Trapped in Cryogenic Matrices

Pierre Rousselot-Pailley, Sophie Sobanska, Nicolas Ferré, and Stephane Coussan

J. Phys. Chem. A, **Just Accepted Manuscript** • DOI: 10.1021/acs.jpca.0c02512 • Publication Date (Web): 22 May 2020

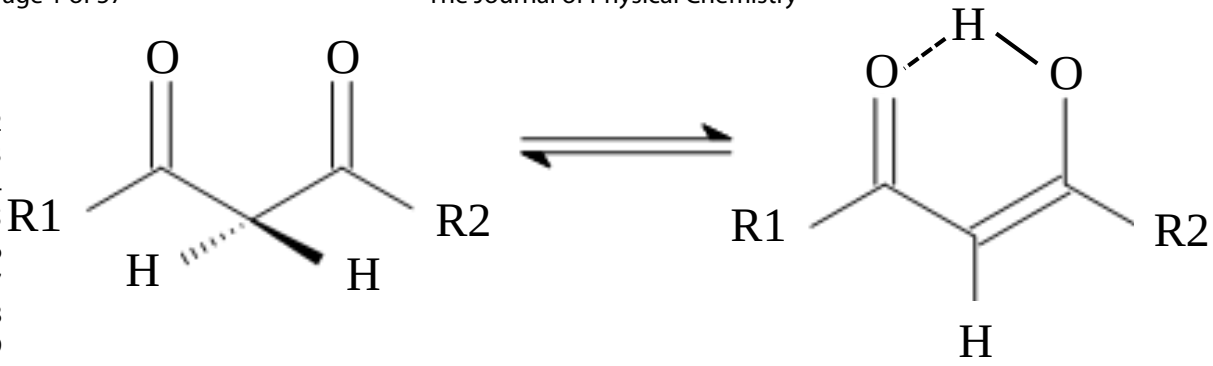

Keto Enol

R1 : H or CH_3

R2 : H or CH_3

CCT$_{OH/CO}$

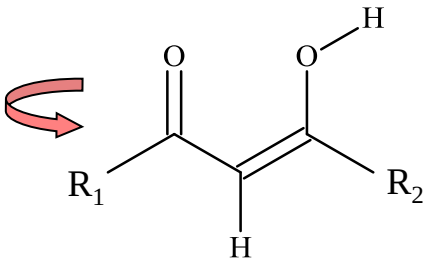

TTC$_{OH/CO}$

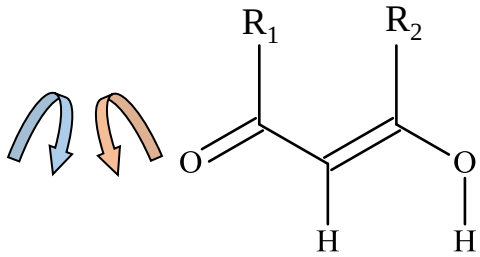

TTT$_{OH/CO}$

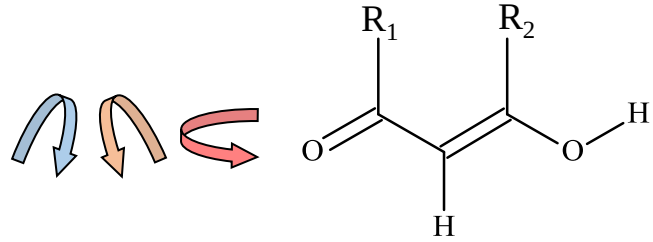

UV

CCC$_{OH/CO}$

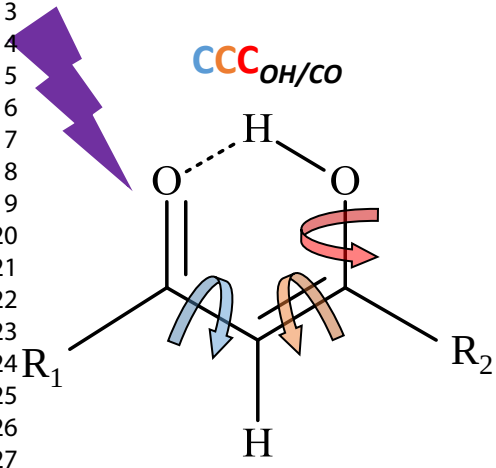

CTC$_{OH/CO}$

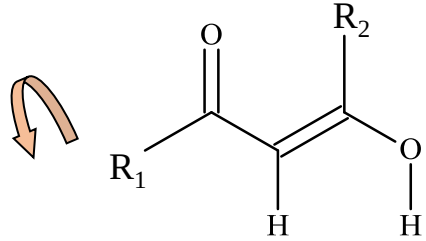

CTT$_{OH/CO}$

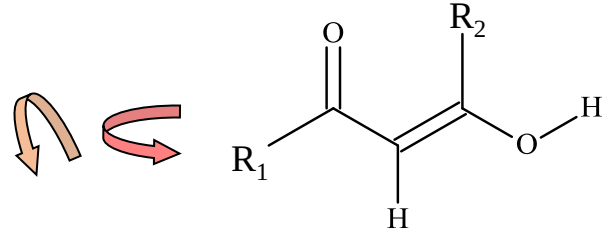

TCC$_{OH/CO}$

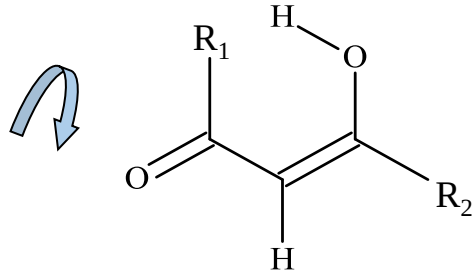

TCT$_{OH/CO}$

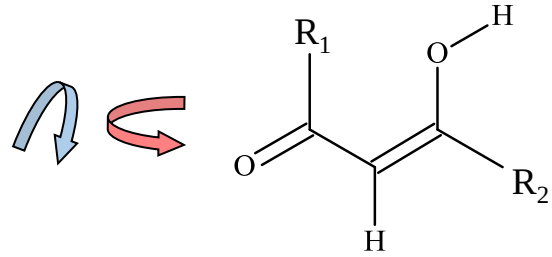

R_1 = H or CH_3

R_2 = H or CH_3

$R_1 \neq R_2$

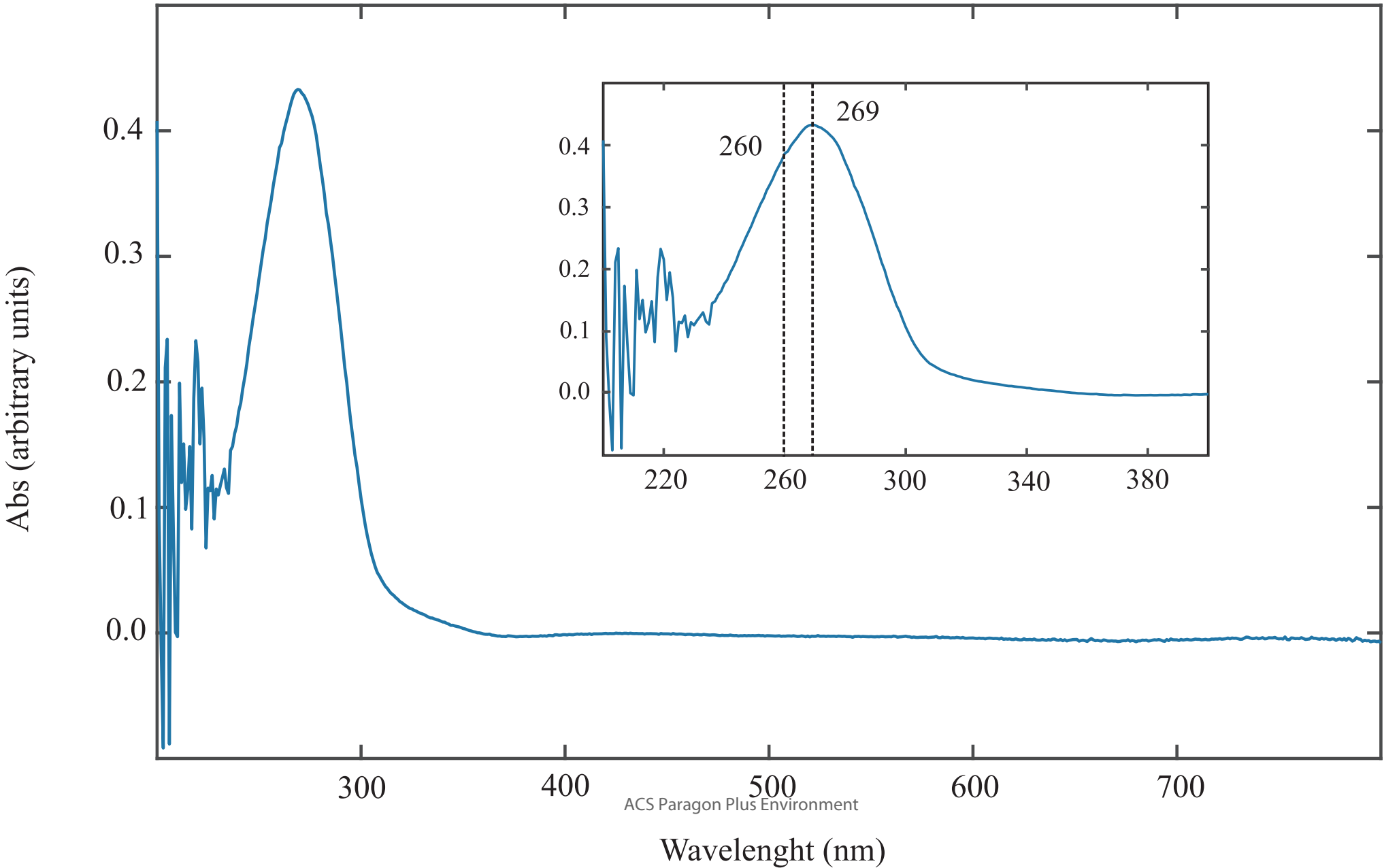
Abs (arbitrary units)
0.4
0.3
0.2
0.1
0.0
300
400
500
600
700
Wavelenght (nm)
269
260
0.4
0.3
0.2
0.1
0.0
220
260
300
340
380

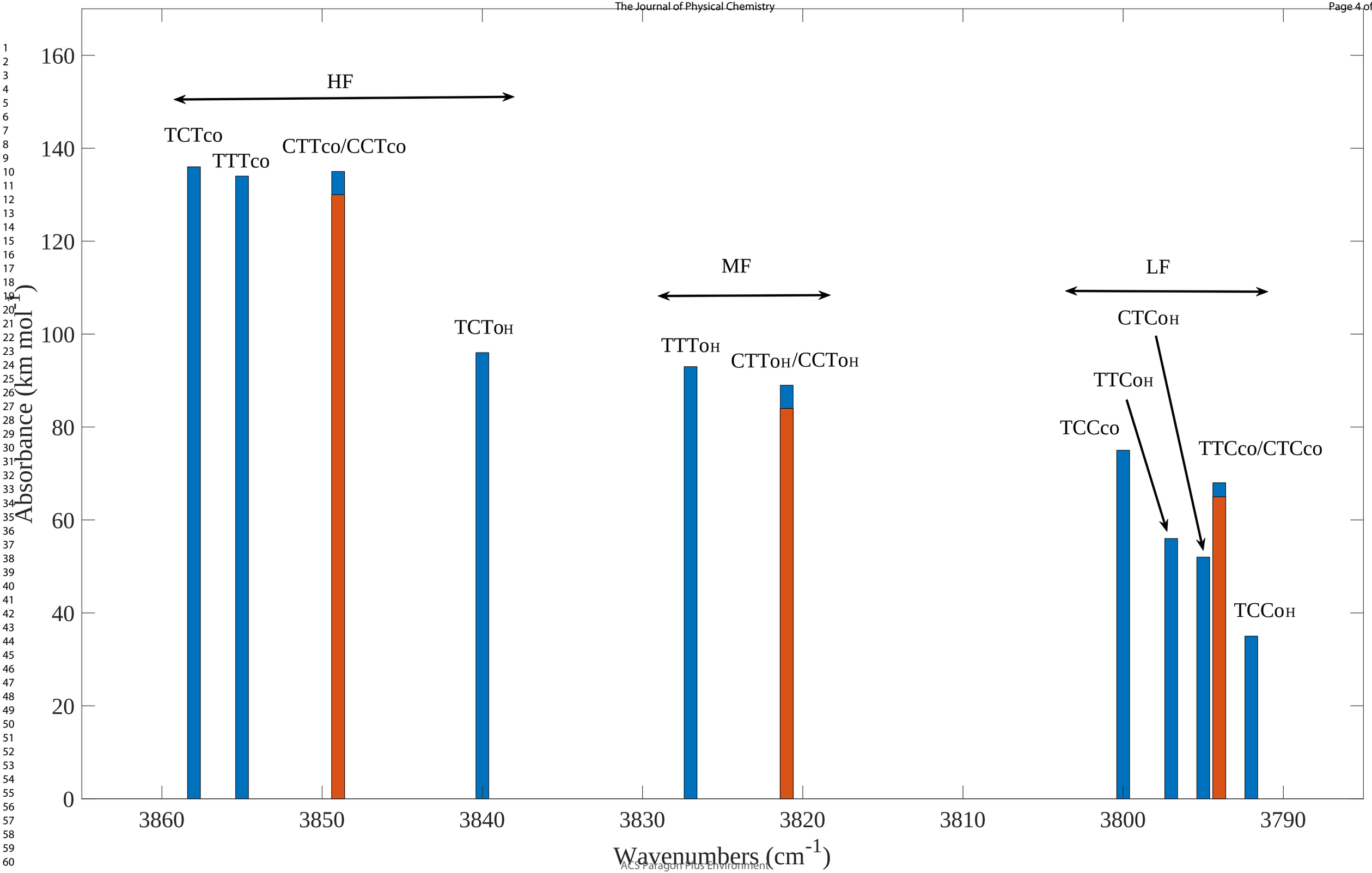
HF
TCTco
TTTco
CTTco/CCTco
TCToн
MF
TTToн
CTToн/CCToн
LF
CTCoн
TTCoн
TCCco
TTCco/CTCco
TCCoн
Absorbance
Wavenumbers (cm-1)
0
20
40
60
80
100
120
140
160
3860
3850
3840
3830
3820
3810
3800
3790

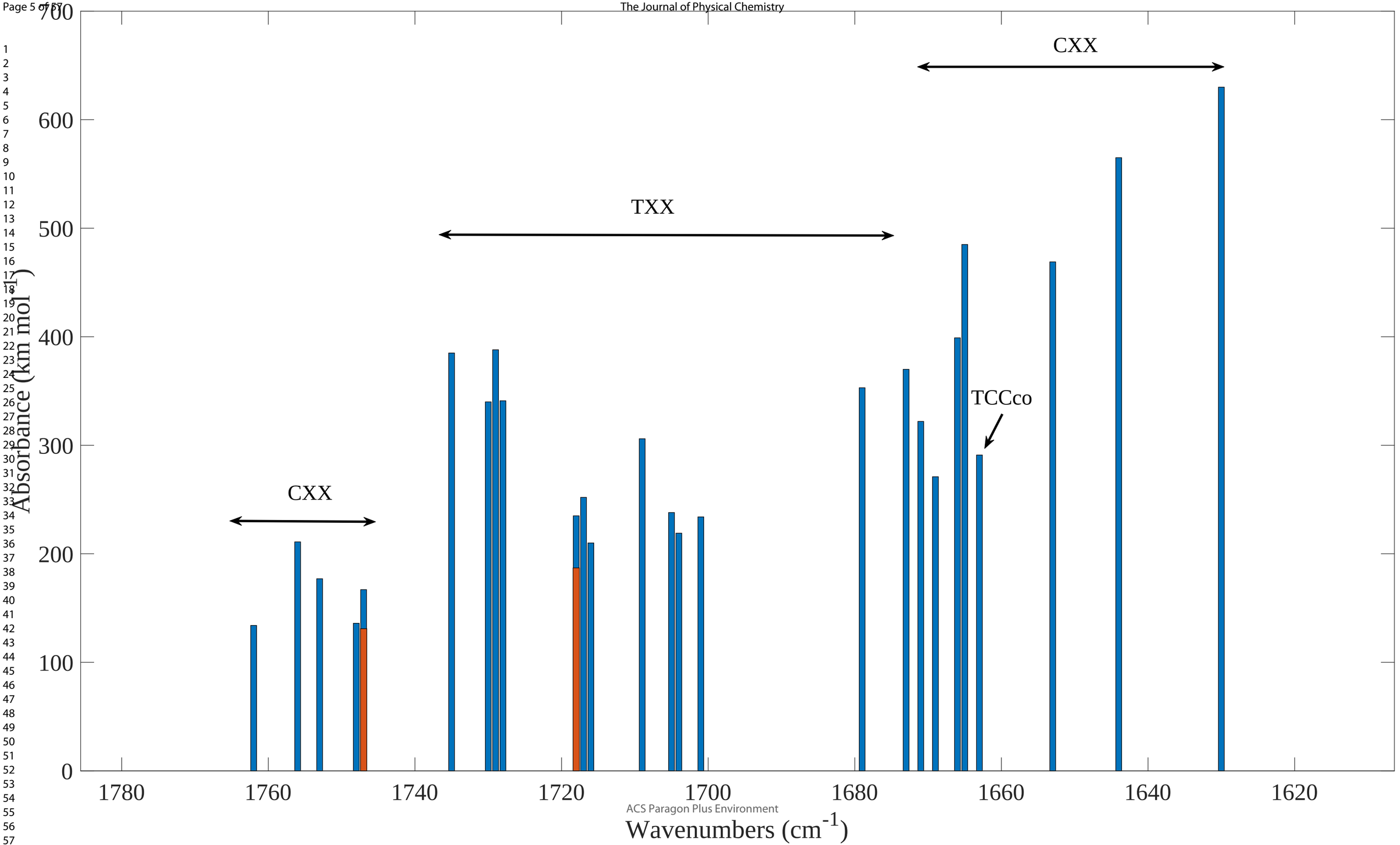
CXX
TXX
CXX
TCCco
Absorbance (km mol^{-1})
700
600
500
400
300
200
100
0
1780
1760
1740
1720
1700
1680
1660
1640
1620
ACS Paragon Plus Environment
Wavenumbers (cm^{-1})

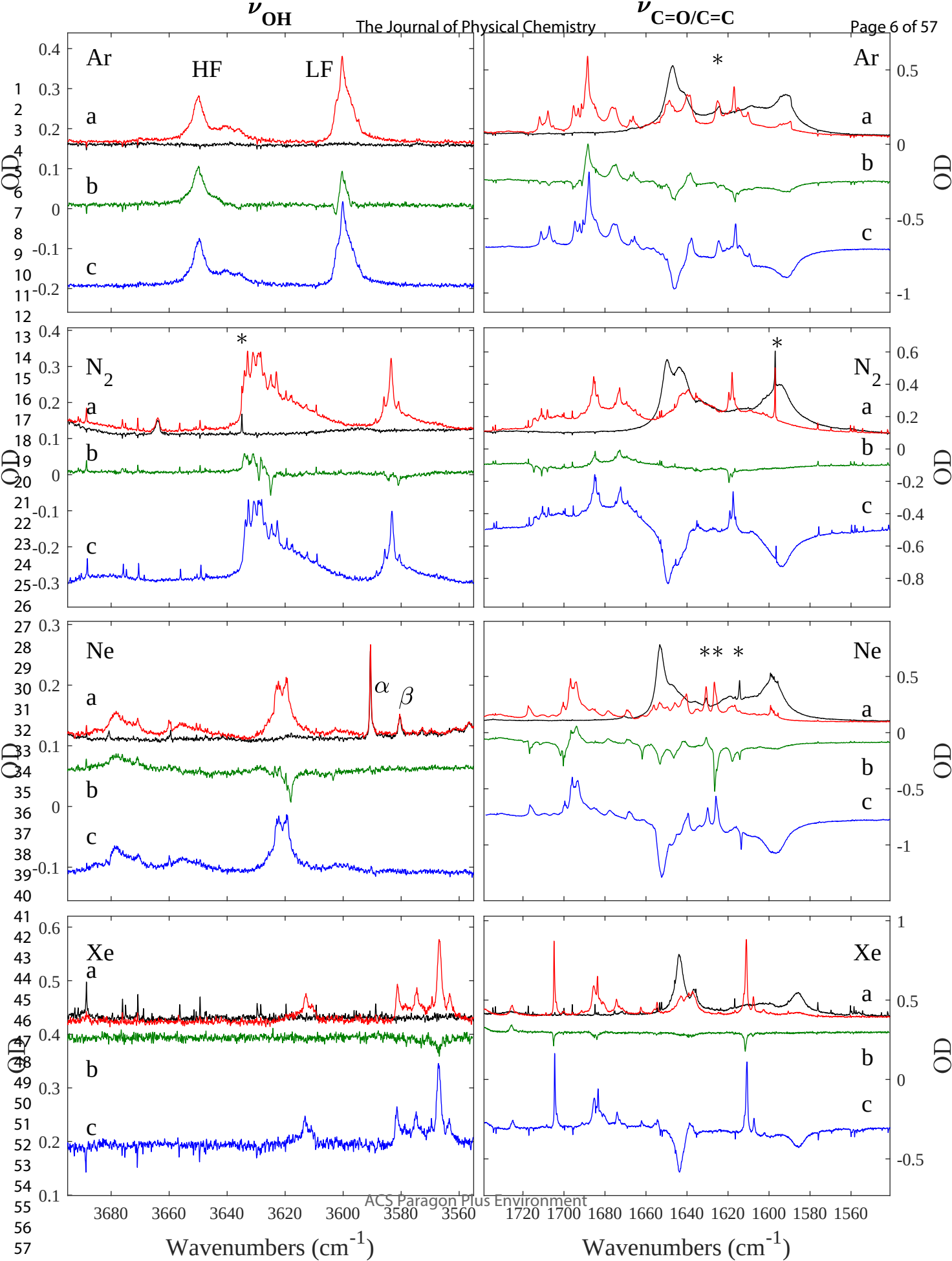
ν_{OH}
$\nu_{C=O/C=C}$
Ar
HF
LF
a
b
c
*
Ar
N2
N2
Ne
α
β
** *
Ne
Xe
Xe
OD
Wavenumbers (cm-1)
Wavenumbers (cm-1)

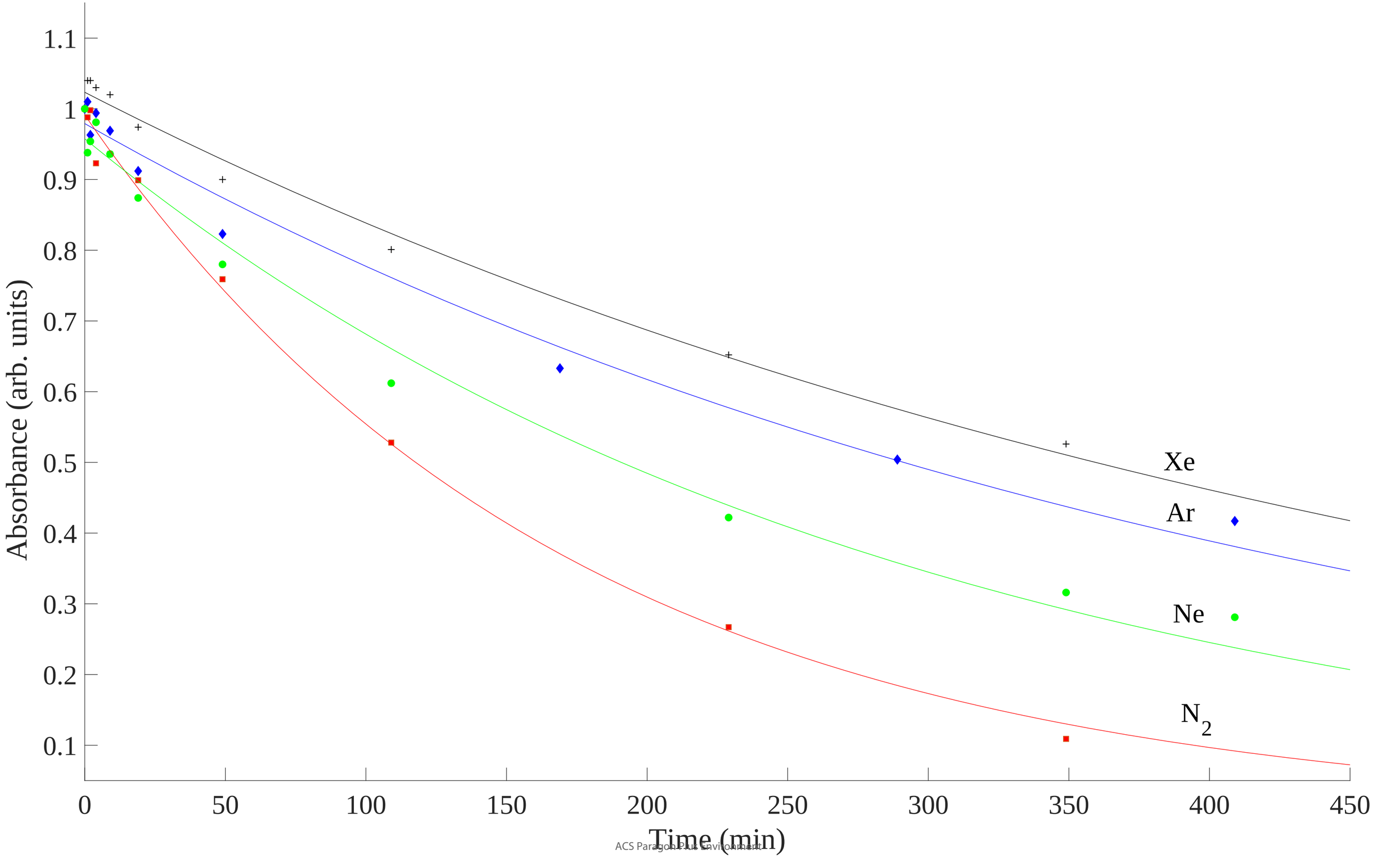
Absorbance (arb. units)
1.1
1
0.9
0.8
0.7
0.6
0.5
0.4
0.3
0.2
0.1
0
50
100
150
200
250
300
350
400
450
Time (min)
Xe
Ar
Ne
N2

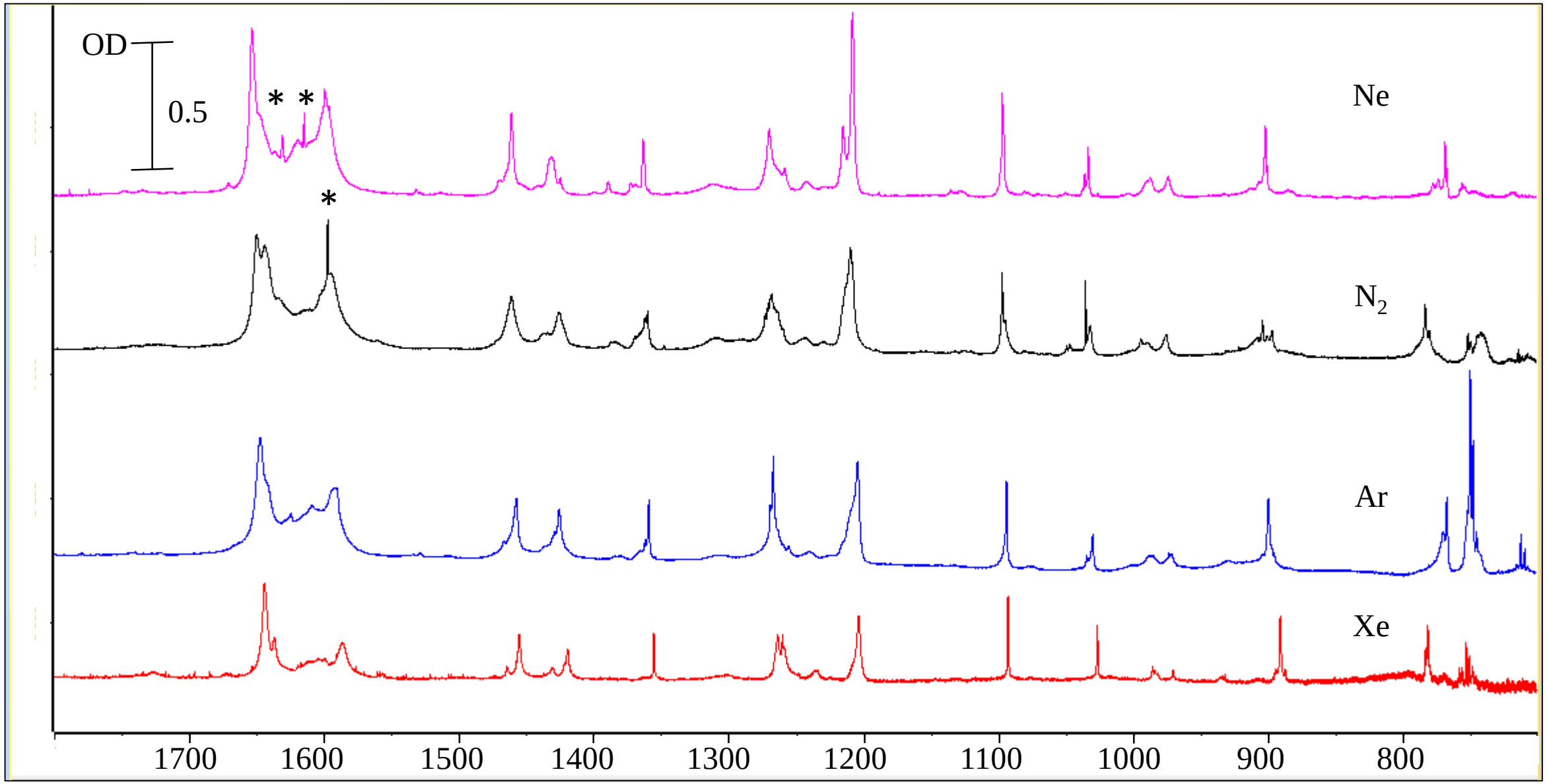
OD
0.5
* *
*
Ne
N2
Ar
Xe
1700
1600
1500
1400
1300
1200
1100
1000
900
800
Wavenumbers (cm-1)

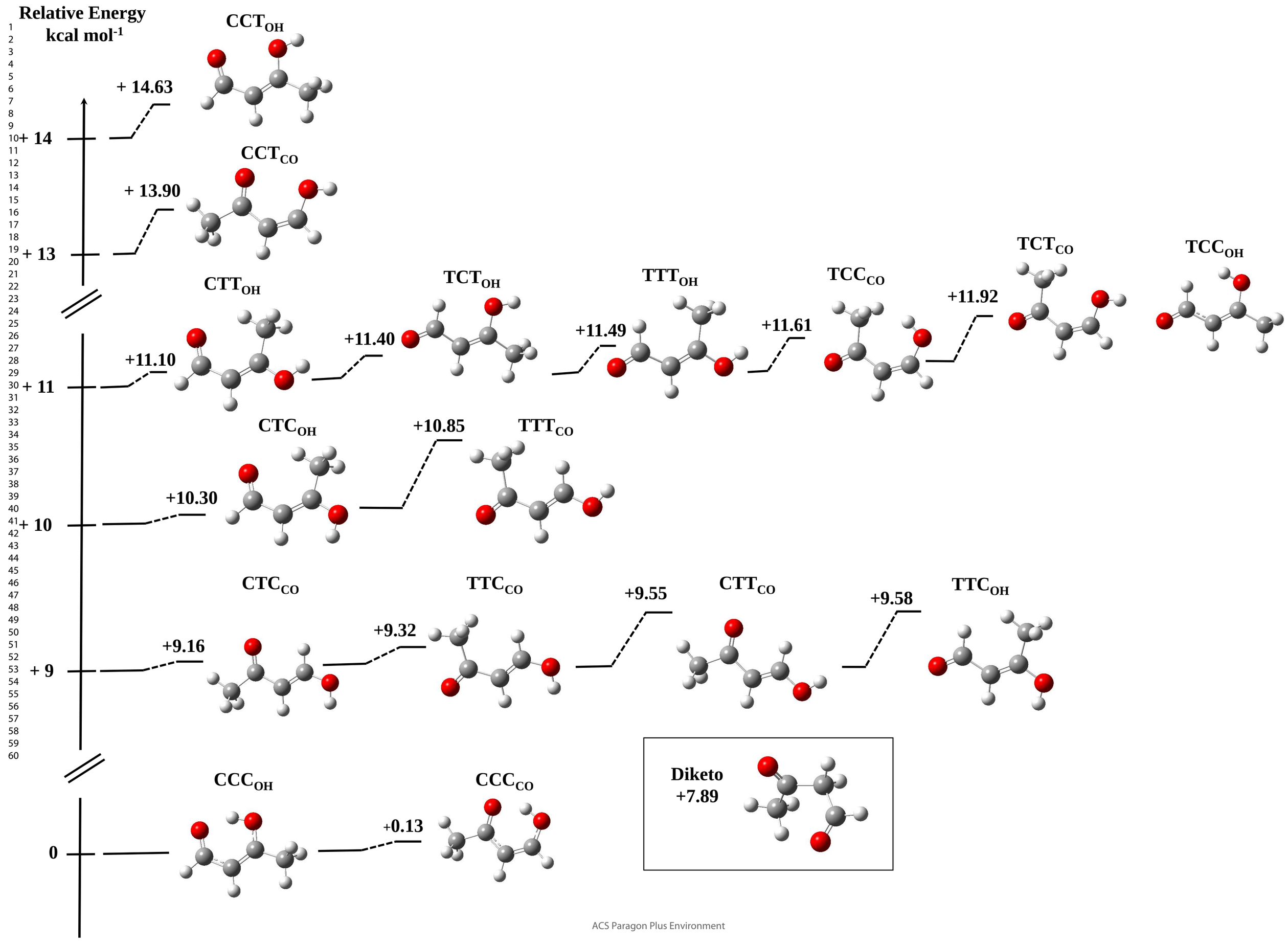
Relative Energy
kcal mol-1
+ 14
+ 13
+ 11
+ 10
+ 9
0
CCTOH
+ 14.63
CCTCO
+ 13.90
CTTOH
+11.10
TCTOH
+11.40
TTTOH
+11.49
TCCCO
+11.61
TCTCO
+11.92
TCCOH
CTCOH
+10.30
TTTCO
+10.85
CTCCO
+9.16
TTCCO
+9.32
CTTCO
+9.55
TTCOH
+9.58
CCCOH
+0.13
CCCCO
Diketo
+7.89

PRP03-109BIS.1.fid
PROTON CDCl3 /opt/topspin3.2 pailley 30

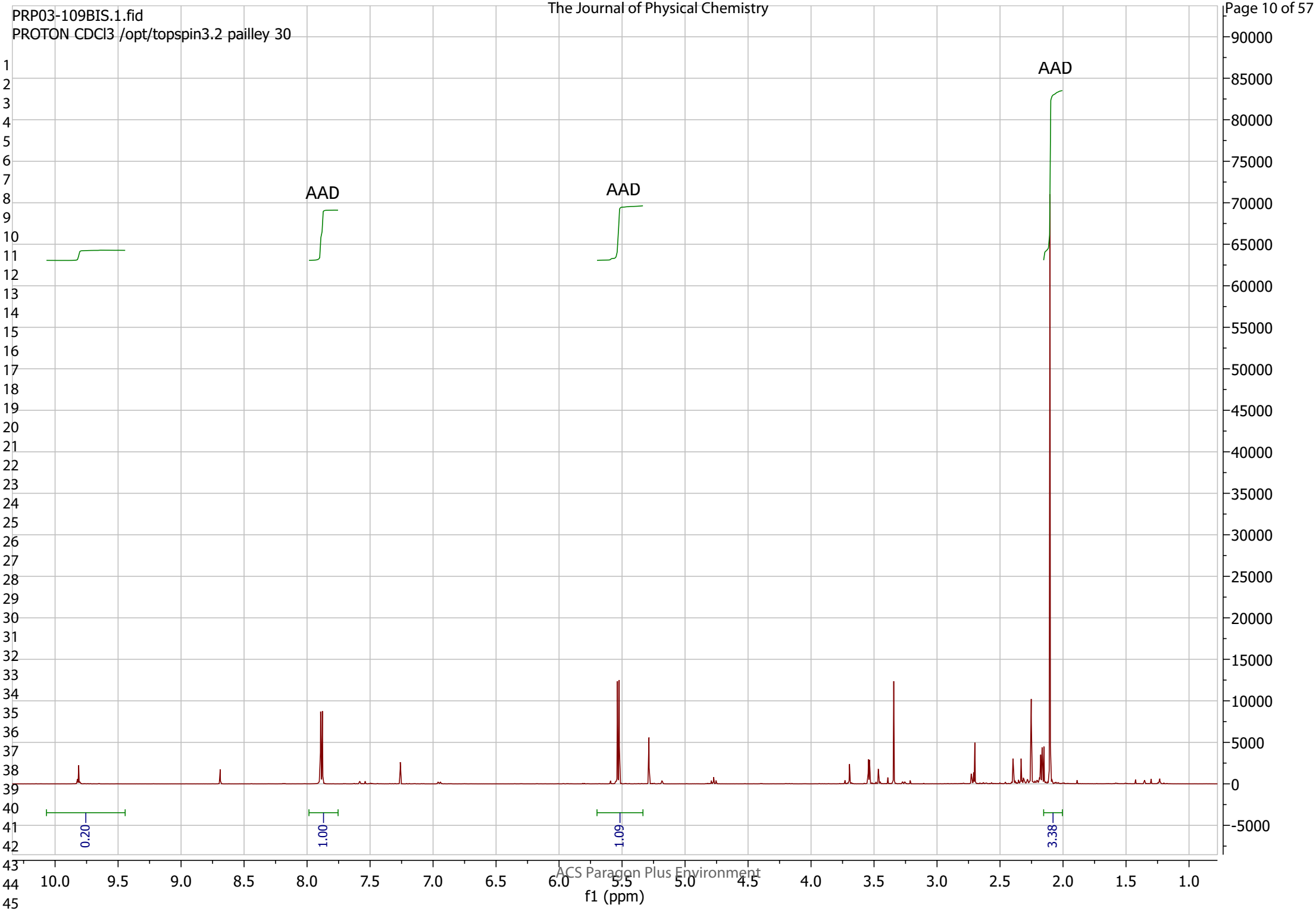

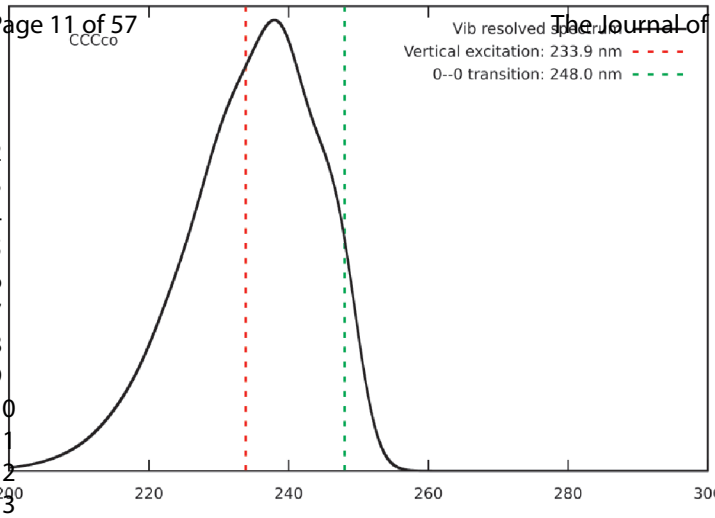

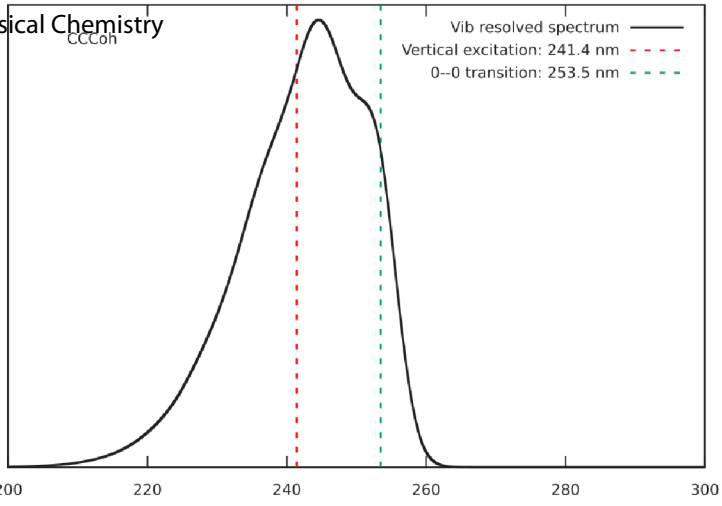

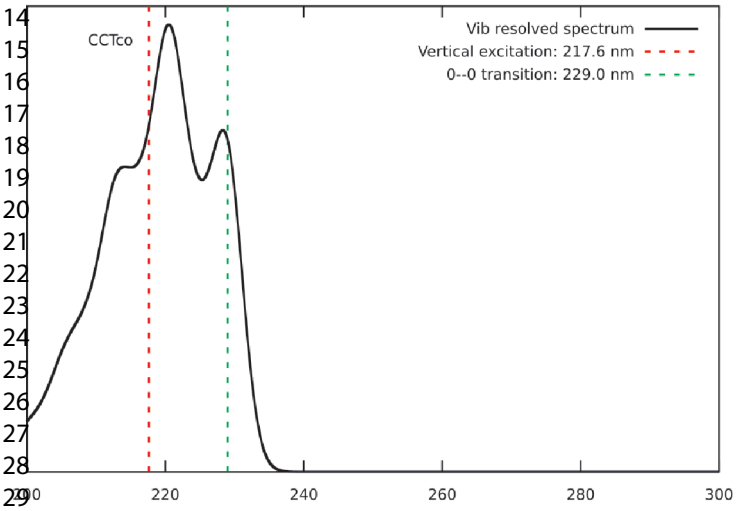

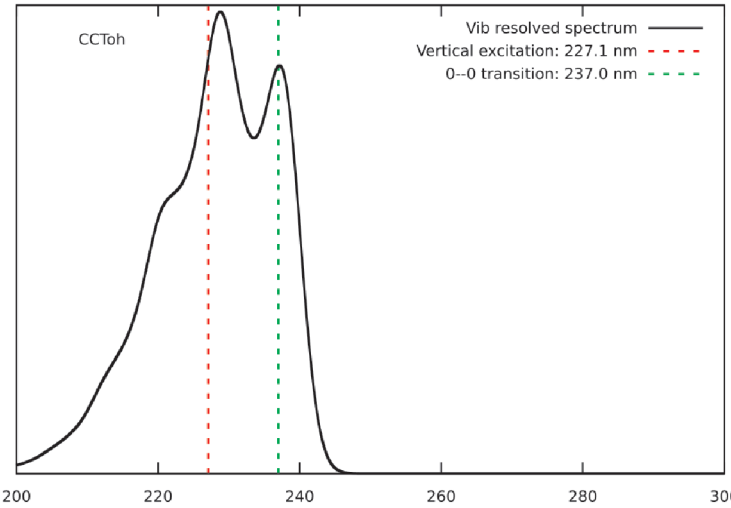

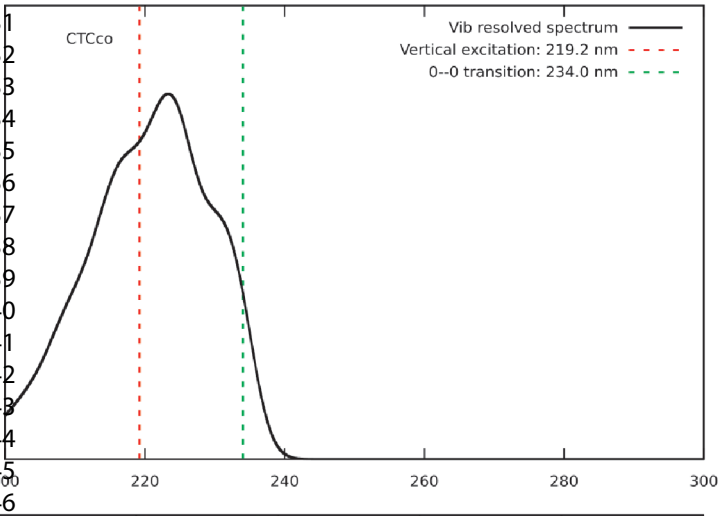

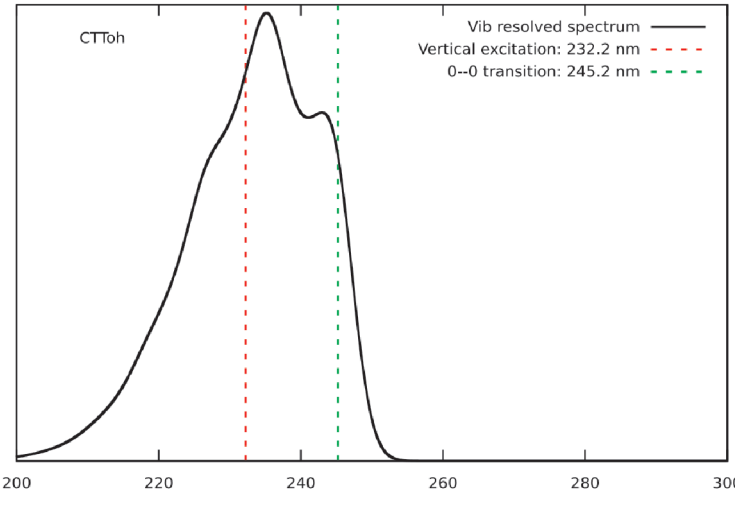

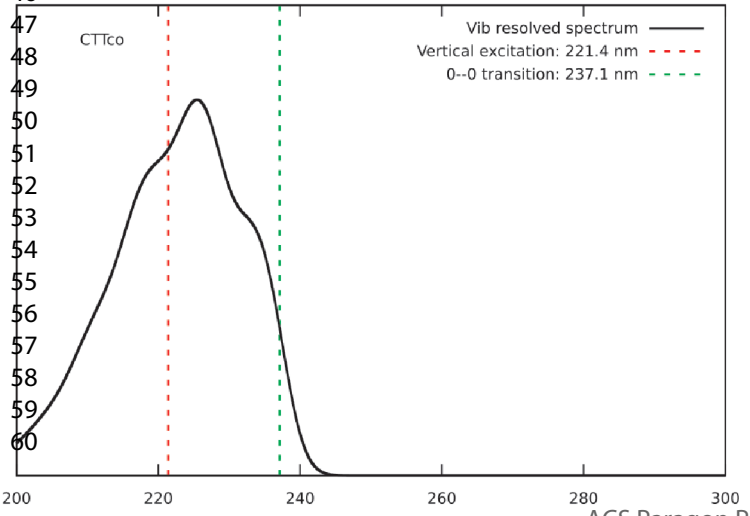

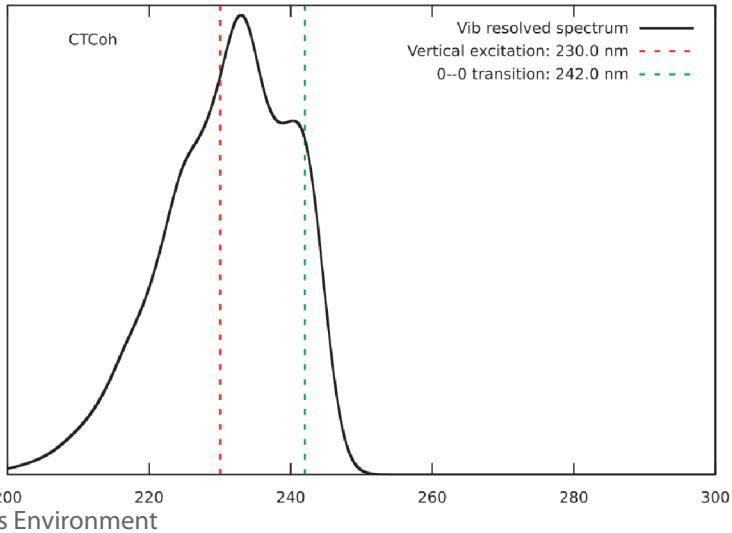

Wavelength (nm)

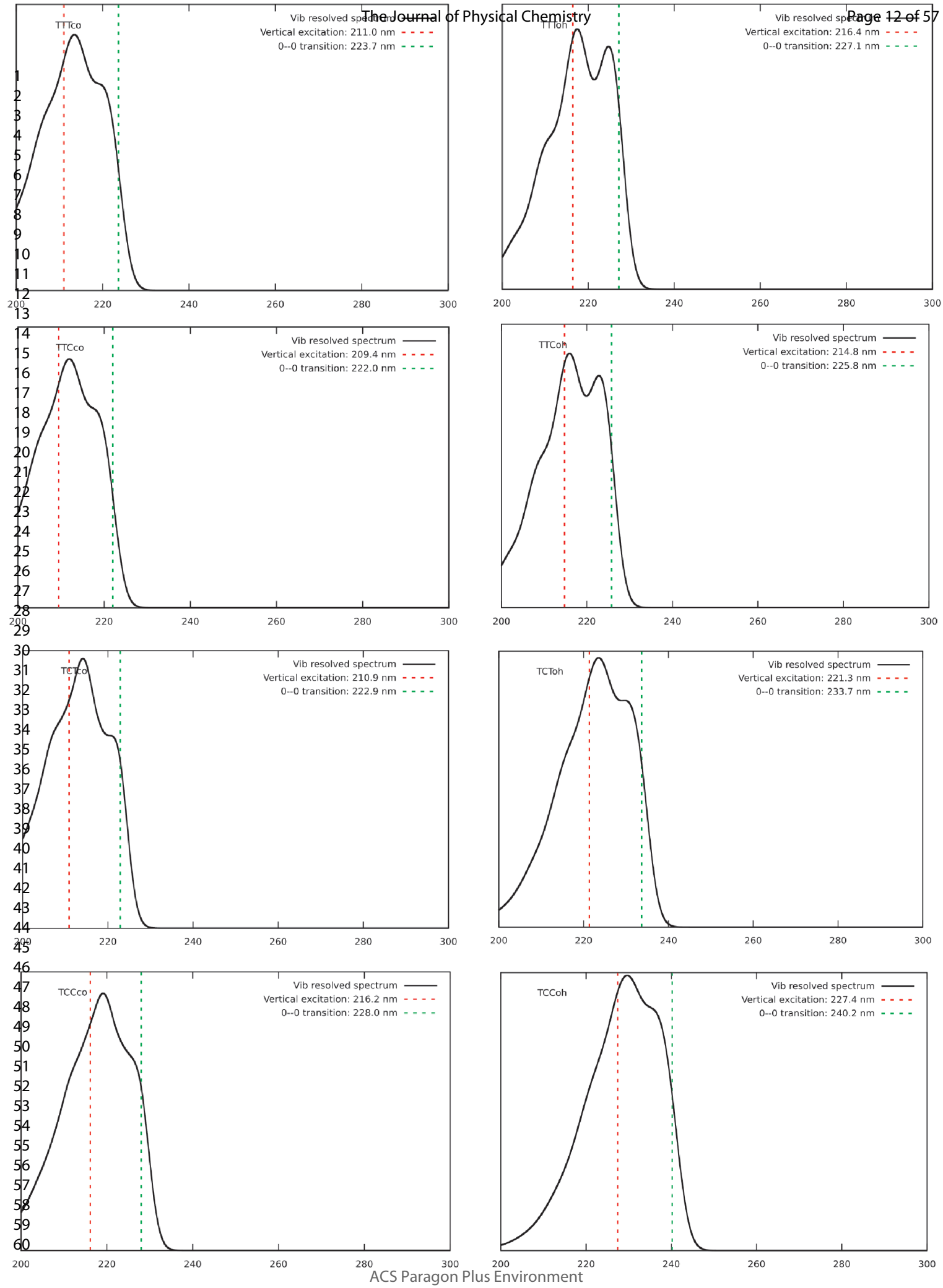
TTTco
Vib resolved spectrum
Vertical excitation: 211.0 nm
0--0 transition: 223.7 nm
TTToh
Vib resolved spectrum
Vertical excitation: 216.4 nm
0--0 transition: 227.1 nm
TTCco
Vib resolved spectrum
Vertical excitation: 209.4 nm
0--0 transition: 222.0 nm
TTCoh
Vib resolved spectrum
Vertical excitation: 214.8 nm
0--0 transition: 225.8 nm
TCTco
Vib resolved spectrum
Vertical excitation: 210.9 nm
0--0 transition: 222.9 nm
TCToh
Vib resolved spectrum
Vertical excitation: 221.3 nm
0--0 transition: 233.7 nm
TCCco
Vib resolved spectrum
Vertical excitation: 216.2 nm
0--0 transition: 228.0 nm
TCCoh
Vib resolved spectrum
Vertical excitation: 227.4 nm
0--0 transition: 240.2 nm
200
220
240
260
280
300
ACS Paragon Plus Environment
Wavelength (nm)

UV Photochemistry of Acetylacetaldehyde Trapped in Cryogenic Matrices

P. Rousselot-Pailley,[†] S. Sobanska,[‡] N. Ferré,[¶] and S. Coussan[*,§]

†*Aix-Marseille Univ, Centrale Marseille, CNRS, iSm2 UMR 7313, Marseille, France*

‡*Institut des Sciences Moléculaires, Université de Bordeaux 1, CNRS UMR 5255, Talence, France.*

¶*Aix-Marseille Univ, CNRS, ICR, Marseille, France*

§*Aix-Marseille Univ, CNRS, PIIM, Marseille, France*

E-mail: stephane.coussan@univ-amu.fr

Abstract

The broad band UV photochemistry of acetylacetaldehyde, the hybrid form between malonaldehyde and acetylacetone (the two other most simple molecules exhibiting an intramolecular proton transfer), trapped in four cryogenic matrices, neon, nitrogen, argon and xenon, has been studied by IRTF spectroscopy. These experimental results have been supported by B3LYP/6-311G++(2d,2p) calculations in order to get S_0 minima together with their harmonic frequencies. On those minima we have also calculated their vibrationnally-resolved UV absorption spectra at the time-dependent DFT ωB97XD/ 6-311++G(2d,2p) level. After deposition, only the two chelated forms are observed while they isomerize upon UV irradiation toward nonchelated species. From UV irradiation effects we have identified several nonchelated isomers, capable, in turn, of isomerizing and fragmenting, even if this last phenomenon seems to be most unlikely due to cryogenic cages confinement. Based on these findings, we have attempted a first approach to the reaction path of electronic relaxation. It appeared

that, as with acetylacetone, the path of electronic relaxation seems to involve triplet states.

Introduction

Acetylacetadehyde (hereafter referred as AAD), is one of the most simple molecules, together with malonaldehyde and acetylacetone (hereafter referred as MA and AA, respectively), exhibiting an intramolecular proton transfer. From our past series of works in cryogenic matrices[1–4] and by comparison with supersonic jet works,[5–7] we put in evidence that in cryogenic matrix, the OH proton is localized, and that the main form present after deposition is the enol one (Figure S1 and Tables 3 and S1). This form is stabilized by a strong internal H-bond, calculated to be of $\approx$ 12 kcal mol^{-1}, in the case of acetylacetone.[8] In "classical" cryogenic matrices, such as nitrogen, argon, neon or xenon, one does not observe the tautomerization between keto and enol forms (Figure 1), while Crépin *et al*[9] induced it by UV (KrF laser) excitation at 248 nm in parahydrogen. Due to the electronic delocalization, the enol forms are rather rigid. However, upon UV irradiation, these forms, also called chelated forms or CCC (see Figure 2), mainly isomerize toward open forms, CXX and TXX (see Figure S2, X = C or T) in matrices,[1–4] while they fragment in molecular beam.[10–13] In Figure S2, the 16 possible AAD isomers are diplayed, where C and T characters stand for *Cis* or *Trans* configurations with respect to C-C, C=C and C-O bonds, respectively. However, due to the assymetry (compared to AA and MA) of AAD, the complexity increases because to one MA/AA isomer corresponds two AAD's, depending on H and -CH_3 positions. OH and CO underscripts stand for -CH_3 position with respect to C=O or OH "side" (Figure S2). AAD's litterature is really scarce. We have found two theoretical works, one at low level of theory deals with isomers geometries and energies,[14] while a second, a lot more sophisticated, and uniquely dedicated to AAD, addresses also tunneling between the two chelated forms, and tautomerization phenomena.[15] Experimentally, a first study of AAD trapped in argon

and xenon matrices has been published by our laboratory many years ago,[16] and two NMR ones.[17,18] The first goal of the present work is to identify if both AAD CCC_{OH} and CCC_{CO} forms are observed, whatever the matrix, after deposition, then, which are the nonchelated isomers present after UV irradiation. Is there a clear difference between the matrices, *i.e.* can we assess if there is a control of the UV photochemistry by the matrix? The second goal of this work is to approach electronic relaxation pathway, like we did for AA and MA.[1–4] On the theoretical point of view, in the case of MA, namely, if numerous theoretical studies have been published on its ground state tunneling effect,[19–21] a lot fewer have addressed that of AA,[22] or MA and AA photochemistries.[23–25] Comparing those latter studies with our experimental results[1–4] we showed that AA electronic relaxation pathway proceeds through T_2 and T_1 states, and that nonchelated forms are those which fragment. On the contrary, in MA case, electronic relaxation proceeds uniquely through singlet states and no fragmentation is observed. So, even the methyl rotators coupling is really weak in AA, this is precisely what induces this electronic relaxation pathways difference with MA. The last goal of this work was thus to guess what is the electronic relaxation pathway of this "hybrid" molecule, in other words, is it the $methyl-methyl$ coupling that governs a relaxation process through triplet states, or is it just the presence of a methyl group that induces this phenomenon?

Experimental

Acetylacetaldehyde Synthesis

The Acetylacetaldehyde was prepared as follow. To 10g of 4,4-Dimethoxy-2-butanone (Acros organics 92%) (75.6 mmole) was added 100mL of HCL 0.5N. The solution was stirred for 72h. After 72h the solution was extracted with 3 × 25mL of methylene chloride. The organic layer was dried over $MgSO_4$ and evaporated under reduced pressure to afford 3g of Acetylacetaldehyde as a yellow oil. The ^1H NMR was recorded on BRUKER Avance III nanobay - 300MHz equipped with a BBFO+ probe. Solvant was $CDCl_3$ (Figure S3). The

UV spectrum was recorded at 298 K (Figure 3), in dichloromethane ([AAD] $\approx$ 0.1 mM L^{-1}), with an Agilent Technologies Cary 60 UV/Vis spectrometer, at 4800 nm/min, with a data interval of 1 nm and an average time of 0.0125 s.

Matrix Experiments

For matrix isolation experiments, AAD was subjected to multiple freeze-pump-thaw cycles under primary vacuum to remove dissolved gases. AAD was then mixed with matrix gases, Ne (N50 grade, Air Liquide), Ar and N_2 (N60 grade, Air Liquide), Xe (N50 grade, Linde), in partial ratio AAD/MG (MG, matrix gas) of $\approx$ 7/1000. Mixtures were deposited onto a gold-platted copper cube cooled to 4.3 K in Ne, 20 K in Ar and N_2, and 40 K in Xe, by a closed-cycle cryogenerator PT-405 from Cryomech compagny. Cryostat and sample-carrier were protected from thermal background radiation by a chrome-platted brass shield kept at $\approx$ 32 K. Controlled heating (Lakeshore Model 336) of the sample carrier was carried out with a 50 Ω resistor, while the background pressure in the vacuum chamber was kept at 10^{-7} mbar by a turbomolecular pump. Fourier transform IR (FTIR) spectra were all recorded at 4.3 K in the reflection mode using a Bruker IFS 66/S spectrometer (resolution: 0.12 cm^{-1}) equipped with a MCT detector. Broad band UV irradiation were carried out with an Oriel high-pressure 500 W mercury lamp (average power: 300 mW, no optical filter, no water filter. For kinetics an average power of 100 mW was used).

Theoretical Calculations

We have carried out two types of theoretical calculations and compared them to those we got in MA and AA cases:[1–4] UV vertical transitions and DFT ground state minima together with their harmonic frequencies sets. Both are presented below.

UV Vertical Transitions

For each isomer, we start by optimizing its geometry in gas phase, using Kohn-Sham Density Functional Theory (DFT), the ωB97XD range-separated exchange-correlation functional[26] and the 6-311++G(2d,2p) basis set. Then, a linear-response Time-Dependent DFT (TD-DFT) calculation is performed to select the lowest electronic excited state with a significant oscillator strength, corresponding to a bright allowed transition which can be described by a $\pi^* \leftarrow \pi$ single excitation. Vertical energy excitation is calculated as the difference between the excited and the ground state electronic energies. The approximate vibrationally-resolved absorption spectrum is obtained using the selected excited state nuclear gradient only, in the Franck-Condon approximation.[27] In other words, both the ground and the selected excited states are assumed to share the same potential energy surface shape. Note that less crude approximations could not be used since the $\pi^* \leftarrow \pi$ excited states do not feature a stable energy minimum geometry (but rather a conical intersection or an avoided crossing with a twisted C=C bond). The resulted absorption spectra have been plotted assuming a 500 cm^{-1} half-width at half-maximum for the convolution.

Theoretical UV Spectra

All the theoretical UV spectra, including vertical excitation and 0-0 transition wavelenghts, are displayed in Figures S4 and S5 and listed in Table 1 (we did not calculate vertical transition of diketo form (displayed in Figure S2), because this latter would just present forbidden $\pi^* \leftarrow n$ ones. All the first allowed $\pi^* \leftarrow \pi$ transitions are $S_2 \leftarrow S_0$. As expected, $CCC_{CO/OH}$ species present the highest wavelenghts because they are the most conjugated ones. In the case of the non-chelated species there is a clear gap between the XXX_{CO} and XXX_{OH} character. Indeed, as clearly displayed in Figures S4 and S5, the XXX_{CO} species present systematically a vertical absorption wavelenghts $\approx$ 10 nm lower than those of XXX_{OH}. It is due to the fact that -CH_3 is electro-donor while -C=O is electro-attractor. As a result when -CH_3 is in close vicinity with -C=O (XXX_{CO} species), this electro-donor

effect is reduced by the attractivity of -C=O, reducing the conjugation and then inducing a shorter vertical excitation value for those latter. It is then convenient to discriminate between three groups:

1. CCC_{CO} and CCC_{OH} with allowed transitions at 241 and 248 nm, respectively.
2. XXX_{CO} nonchelated species with allowed transitions ranging between 209 and 221 nm.
3. XXX_{OH} nonchelated species with allowed transitions ranging between 215 and 232 nm.

Even the theoretical method used in this work is not the one we used for MA and AA,[1,3] we get comparable vertical excitation values for AAD XXX_{OH}, MA and AA isomers. It is due to the fact they present comparable conjugated systems. We can then use confidently the same UV broad band irradiation experimental process to discriminate between all the $XXX_{CO/OH}$ acetylacetaldehyde isomers, because all these species should present close UV experimental spectra.

DFT Calculations

Calculations have been performed at the B3LYP/6-311++G(2d,2p) level of calculation, using the GAUSSIAN 16 computer code[28] and the basis set 6-311++G(2d,2p) of Pople *et al.*[29,30] Becke's[31,32] three-parameters functional was used, including the gradient-exchange correction and the non local correlation function of Lee, Yang and Parr.[33]

In Figure S2 is displayed all the minima with their relative energies compared to that of CCC_{OH} one. To each MA or AA nonchelated isomers correspond two AAD ones, depending on terminal -H and -CH_3 group positions. We have chosen to call them XXX_{CO} and XXX_{OH} with respect to the methyl position, C=O side or O-H one. If we compare those relative energies with those found, at the same level of calculation, for MA[1] or AA,[34] we notice that AAD presents an intermediate situation between MA, for which TTC is located 6.7 kcal mol^{-1} above CCC, and AA for which CTC is located 11.1 kcal mol^{-1} above CCC (TTC and

CTC are the most stable nonchelated isomers with respect to their relative CCC MA and AA parents molecules, respectively). In the same trend, the highest nonchelated energy is seen to be those of CCT(MA) at 12.8, CCT_{OH}(AAD) at 14.6 and TTT(AA) at 16.6 kcal mol^{-1}, respectively. Is it so surprising? It seems that the energy gap with respect to the chelated forms, increases with the number of methyl groups. Those latter induce a larger distortion in AA case, namely for TTT and TTC which exhibit a *syn-1,3 methyl-methyl* interaction, while CCT, because of sp^2/sp^3 oxygen lone pairs interaction is the most energetically disfavoured isomer in both MA and AAD cases.

Considering our past works on AA and MA,[1,2] we should be able to observe all the nonchelated forms excepted $CCT_{OH/CO}$. Indeed, those two latters display a sp^2/sp^3 oxygen lone pairs interaction which avoids their observation, at our recording timescale (s), before they relax towards more stable ones. However, from calculated frequencies, namely in the ν_{OH} and $\nu_{C=O}/\nu_{C=C}$ regions (those in which isomers present clear spectral differences) (Table 2), we can guess that many bands will overlap, rendering uneasy an unambiguous vibrational assignment to one or another isomer. A first step will be to identify groups of bands belonging to CXX or TXX species.

Theoretical IR Spectra

As in the case of MA and AA,[1,2] we have chosen ν_{OH} and $\nu_{C=O}/\nu_{C=C}$ (Table 2) regions because non-chelated isomers present, in those ones, typical sets of bands. Studying those regions would allow us to discriminate between CXX and TXX species.

ν_{OH} Region (Figure 4). $CCC_{OH/CO}$ ν_{OH} modes are calculated at 3218.3 and 3215.1 cm^{-1}, respectively, with normalized intensities given to be 0.0. Adding the fact, that as in the case of MA and AA,[1,2] due the strength of the internal H-bond,[8] these bands should be spread over hundreds of wavenumbers, we do not expect to observe them. With regards to nonchelated isomers, we can conveniently discriminate between three groups:

1. A high frequency (HF) group containing TCT_{CO}, TTT_{CO}, CTT_{CO}, CCT_{CO} and TCT_{OH},

with bands centered at 3858.0, 3854.8, 3849.4, 3848.7 and 3840.3 cm^{-1}, respectively.

2. A medium frequency (MF) group containing TTT_{OH}, CTT_{OH} and CCT_{OH}, with bands centered at 3827.4, 3821.1 and 3821.8 cm^{-1}, respectively.

3. A low frequency (LF) group containing TTC_{OH}, TTC_{CO}, TCC_{OH}, TCC_{CO}, CTC_{OH} and CTC_{CO} with bands centered at 3797.5, 3793.8, 3791.8, 3800.1, 3795.1 and 3794.5 cm^{-1}, respectively.

It is interesting to note that couples $TTC_{OH/CO}$, $TTT_{OH/CO}$, $CTT_{OH/CO}$ and $CCT_{OH/CO}$ are spread over HF and MF regions, *CO* character being only HF while *OH* is MF. The three last couples $TTC_{OH/CO}$, $TCC_{OH/CO}$ and $CTC_{OH/CO}$, are uniquely LF. Those latters present frequency splits (frequency gap between OH and CO ν_{OH} modes of each AAD isomer) of $\approx$ 4 (TTC), 8 (TCC) and 1 (CTC) cm^{-1}, while between HF and MF bands, the splits are of $\approx$ 27 (TTT), 18 (TCT), 28 (CTT) and 27 (CCT). As a result it could be uneasy to identify unambiguously LF species because of the experimental overlapping.

$\nu_{C=O}/\nu_{C=C}$ Region (Figure 5). CCC_{OH} and CCC_{CO} $\nu_{C=O}/\nu_{C=C}$ modes are calculated at 1646.2 and 1679.5 cm^{-1} ($\Delta\nu = 33.3\,cm^{-1}$), and 1630.0 and 1683.4 cm^{-1} ($\Delta\nu = 53.4\,cm^{-1}$), respectively. As in the case of MA and AA,[1,2] $\nu_{C=C}$ mode is calculated to be higher than that $\nu_{C=O}$. It is a direct consequence of the strong internal H-bond which induces this strong $\nu_{C=C}$ blue shift. The average normalized intensity of these modes is $\approx$ 0.45. They should be the most intense bands of the spectrum. For nonchelated species, this region is one of the most salient to discriminate among themselves. As for CCC, those bands should be the most intense of their spectra. However, due to the existence of possibly non less than 16 isomers, *i.e* 32 bands, spread over 130 cm^{-1}, it could result a strong experimental overlapping. As in the ν_{OH} region we can conveniently separate them by their $\Delta\nu = |\nu_{C=O} - \nu_{C=C}|$ (Table 2) and the relative positions of their bands.

1. The first groups contains $CTT_{OH/CO}$, $CTC_{OH/CO}$ and $CCT_{OH/CO}$ couples which should display $\Delta\nu$ ranging from 87.0 cm^{-1} to 116.4 cm^{-1}. As displayed in Figure 5, and in

Table 2, the bands of this group are supposed to surround those of the others non-chelated isomers.

2. The second group contains $TCC_{OH/CO}$ and $TTC_{OH/CO}$ couples which should display $\Delta\nu$ of 55.2, 39.1, 63.9 and 54.6 cm^{-1}, respectively.

3. The third group contains $TCT_{OH/CO}$ and $TTT_{OH/CO}$ couples which should display $\Delta\nu$ of 24.4, 12.1, 28.5 and 9.2 cm^{-1}, respectively.

Even the study of these regions should be enough to discriminate between non-chelated isomers, others typical sets of bands could be used to support the vibrational assignments, namely in the 1500-900 cm^{-1} range (for example CTC_{CO} should display a normalized intensity (on CTC_{OH} $\nu_{C=C}$ mode) 0.5 band centered at 1140.9 cm^{-1}, and TTT_{OH} a 0.5 normalized intensity band centered at 1207.8 cm^{-1}).

Experimental Results and Discussion

UV spectroscopy

The experimental spectrum of AAD in dichloromethane at 298 K is displayed in Figure 3. One is able to observe only one band centered at 269 nm, with a shoulder at 260 nm, which should be those of CCC_{OH} and CCC_{CO} species, respectively, almost the only forms present before UV irradiation, in cryogenic matrices[1,2] and in solution. However, we cannot discard the presence of a few amount of diketo form even this form is energetically strongly disfavoured with respect to the enol one. Considering that 1 kcal mol^{-1} $\approx$ 503.2 K, the thermal bath at 298 K does not bring enough energy to isomerize CCC species toward diketo form or the nonchelated ones, the closest being calculated to range between 9 and 10 kcal mol^{-1} above CCC species (Figure 2). Unfortunately we have not been able to record this spectrum at 4 K, in the four matrices. As a result we are not able to present nonchelated species one. However, one can retrieve some insights from this spectrum. From theoretical

results, one could expect for CCC species two bands of almost the same intensity separated by about 6 nm. Indeed, the two CCC species are almost the same energy (Figure 2), and present almost the same oscillator strength for their two first allowed $S_2 \leftarrow S_0/\pi^* \leftarrow \pi$ transitions (Table 1), *i.e.* 0.2353 against 0.2717 for CCC_{CO} and CCC_{OH}, respectively. Experimentally we observe a 9 nm difference between the top of the band and the shoulder. Is it so surprising that expecting two isomers, we observe a quite symetrical band? MA and AA are known to exchange the enol proton in gas phase and in liquid, leading to a splitting of the ground state.[5,6,19–21,35,36] It could be what happens here: we observe a kind of average situation in which proton is exchanged and concomitantly it remains enough forms of each CCC isomer to structure the band with this shoulder. It should also be noted that even this UV spectrum has been recorded in dichloroethane, at room temperature, the 269 nm band for CCC matches with those of MA and AA chelated forms, at 269-275 and 265-269 nm, respectively.[1,2]

IR spectroscopy - Broad band UV irradiations

The effects of UV broad band irradiation in the four cryogenic matrices are displayed in Figure 6. The full vibrational spectrum of CCC_{XX} chelated isomers in the four matrices is given in Figure S1. Neither ν_{OH} region is displayed because these bands are not observable (see text below), nor ν_{CH} which presents weak bands ranging between 3090 and 2650 cm^{-1}. Experimental frequencies of the two chelated forms are gathered in Tables 3 and S1.

Argon Matrix. Before irradiation, one observes no ν_{OH} CCC band, because these bands, calculated at 3218.3 and 3215.1 cm^{-1}, for CCC_{OH} and CCC_{CO}, respectively, are certainly spread over hundreds of wavenumbers,[37] and their normalized intensities are calculated to be 0 (Table 2). It is due to the internal H-bond strength, calculated to be 12 kcal mol^{-1}, in the AA case.[8] In the other hand, broad multiplets are observed at 1648.7-1647.0-1641.5 and 1608.2-1602.8-1594.3-1591.1 cm^{-1}. If we consider the most intense band of each multiplet,

i.e. 1647.0 and 1591.1 cm^{-1}, it leads to a $\Delta\nu$ of $\approx$ 56 cm^{-1}. Comparing this latter $\Delta\nu$, with those theoretical (Table 2), we can assign it to CCC_{CO}, while those at 1641.5 and 1608.2 cm^{-1} (*i.e.* $\Delta\nu \approx 33$ cm^{-1}), which are surrounded by the two formers, could be assigned to CCC_{OH} ((Table 3). After 500 min of irradiation, one observes new band groups in the ν_{OH} region: one, HF-MF, presents bands ranging between 3660 and 3630 cm^{-1}, the other, LF, between 3605 and 3590 cm^{-1}. These bands are due to nonchelated isomers. In the $\nu_{C=O/C=C}$ region, one observes multiplets growing with strongest bands located at 1711.9, 1707.8, 1695.3, 1688.5, 1625.4, 1617.0 and 1615.2 cm^{-1} (Tables 4 and 5). At this stage, it is impossible to discriminate between nonchelated isomers candidates for these spectral features. However, if we consider the position of these multiplets we can confidently assume the presence of CXX and TXX species. But which ones? Are we able to go further into the identification of those nonchelated isomers? One observes that after 60 min irradiation, some nonchelated bands start to decrease in favor of other nonchelated ones (there could also be a back conversion toward CCC, but as it continues to be consumed, we are unable to identify it). In Figure 6, Ar (trace (c)) shows difference between spectrum after 500 min irradiation minus spectrum after deposition, when photostationnary state is reached, and spectrum after 500 min irradiation minus after 60 min irradiation (trace (b)), *i.e.* time from which inter nonchelated isomerization is observed. In the ν_{OH} region 3640.0, 3636.2, 3602.4 and 3597.3 cm^{-1} bands decrease while 3649.8, 3649.1, 3600.3, 3599.4 and 3598.3 cm^{-1} increase. In the $\nu_{C=O/C=C}$ region, two groups of bands decrease, the first group contains 1712.2, 1707.8, 1695.5 and 1691.4 cm^{-1} bands and the second one contains those centered at 1625.2, 1621.1, 1616.9 and 1615.3 cm^{-1}. These decreases are counterbalanced by four sets of increasing bands at 1689.3, 1688.6, 1686.6, 1685.2, then 1676.8, 1675.0, then 1667.7, 1666.3, then 1640.0 and 1638.4 cm^{-1}. Therefore, decreasing and increasing nonchelated isomers present following spectral features:

1. Decreasing ν_{OH} bands are MF and LF while decreasing $\nu_{C=O/C=C}$ ones present $\Delta\nu$ ranging between 68 and 97 cm^{-1}. Moreover, those latters surround increasing ones.

2. Increasing ν_{OH} bands are HF and LF while $\nu_{C=O/C=C}$ ones present multiplets, whose average positions are peaked at 1687, 1676, 1667 and 1639 cm^{-1}, *i.e.* separated by $\Delta\nu$ ranging from 9 to 48 cm^{-1}. This distribution fits well with that theoretical displayed in Figure 5. From Table 2 and Figure 5, we can confidently assume that these ν_{OH} and $\nu_{C=O/C=C}$ increasing bands are due to TXX species.

The combination of MF and LF ν_{OH} decreasing bands with $\nu_{C=O/C=C}$ $\Delta\nu$ ranging between 68 and 97 cm^{-1} leads us to assign those signals to CXX, TCC_{OH} and TTT_{OH} species. Indeed, with $\Delta\nu$ ranging between 68 and 97 cm^{-1} with bands surrounding the other nonchelated ones, the decreasing species are unambiguously CXX with the exception of TCC_{OH} and TTT_{OH} (Table 2). However, we can discard the presence of CCT species because of the strong $sp^3 - sp^2$ electron lone pairs repulsion (Figure S2), and by the fact we do not observe $\nu_{C=O}$ bands blue-shifted by $\approx$ 3 and 9 cm^{-1} with respect to that at 1712.2 cm^{-1} (tentatively assigned to CTT_{CO}, see below). This assumption is highly supported by the fact CCT species have never been observed in our past works on AA and MA.[1,2] We assign the two decreasing bands at 1695.5 and 1691.5 cm^{-1} to TCC_{OH} and TTT_{OH}, respectively, because they belong to typical TXX_{OH} multiplets, and because of the two decreasing OH bands at 3640.0 (MF) and 3597.3 (LF) cm^{-1} which are also TXX. In one hand, there is only one TXX MF species (which should display a blue-shifted ν_{OH} band with respect to CTT_{OH}, $\Delta\nu \approx 6$ cm^{-1}), with a $\nu_{C=O}$ frequency at 1691.5 cm^{-1}, red-shifted by about 4 cm^{-1} with respect to the highest $\nu_{C=O}$ TXX band, it is TTT_{OH}. In the other hand, the lowest calculated ν_{OH} frequency is that of TCC_{OH} which also presents the highest (TXX) $\nu_{C=O}$ one. This is why we have assigned the 3597.3 and 1695.5 cm^{-1} bands to TCC_{OH}. In the same way, CTT_{CO} species should present a HF ν_{OH} band that we do not observe because the TXX HF bands overlap it, but the presence of the band at 1712.2 cm^{-1}, the highest we observe in the $\nu_{C=O}$ region clearly indicates its presence. Another strong argument in favor of the identification of those six isomers is the fact they are calculated to absorb at roughly the same wavelenght (Table 1), *c.a.* 232, 221, 230, 219, 231 and 227 nm for CTT_{OH}, CTT_{CO}, CTC_{OH},

CTC_{CO}, TCC_{OH} and TTT_{OH}, respectively. It makes thus sense, that if these species absorb at roughly the same wavelenght, they should display the same behaviour upon UV irradiation. What about TCT_{OH} and TTC_{OH} which are calculated to absorb both at 221 nm? We should also see them decrease. From Table 2, they present almost degenerated ν_{CO} mode with TTT_{OH} (1729.7 and 1728.4 cm^{-1}, respectively) while they should be HF and LF in the ν_{OH} region, respectively. If one considers that XXX_{OH} species (mainly) are consumed from 60 min irradiation, and the fact XXX_{CO} ones present UV transitions lower than those former (excepted CCT_{CO}, CTC_{CO} and CTT_{CO}, Table 1), we should mainly observe inter $XXX_{OH} \rightarrow XXX_{OH}$ and $XXX_{OH} \rightarrow XXX_{CO}$ isomerizations. Moreover, at the same time $CCC_{OH/CO}$ is still consumed giving $XXX_{OH/CO}$ isomers. One relevant example is the observation of multiplet growing at 1689.3, 1688.6 and 1686.6 cm^{-1}, which is typical of TXX_{OH} isomers. This is why we can assign this multiplet to TCT_{OH}, which is ν_{OH} HF (calculated to be blue-shifted by $\approx$ 19 cm^{-1} with respect to CTT_{OH}, against 13 cm^{-1} experimentally) and to TTC_{OH} which is ν_{OH} LF (calculated to be blue-shifted of $\approx$ 6 cm^{-1} with respect to TCC_{OH}, against 3 cm^{-1} experimentally). The two growing multiplets peaked at 1676 and 1667 cm^{-1} should be associated to TTT_{CO} and TCT_{CO} while TTC_{CO} and TCC_{CO} present degenerated $\nu_{C=O}$ modes with those two latters (multiplet at 1676 cm^{-1}). The last multiplet peaked at 1639 cm^{-1} can be associated with TTC_{CO} and TTC_{OH}. To summarize the UV broad band irradiation effects observed in Ar matrix, $CCC_{OH/CO}$ chelated forms are the only forms present after deposition, while upon broad band UV irradiation, those latters isomerize toward all nonchelated forms excepted $CCT_{OH/CO}$ species which are not identified (at our timescale). We could suggest some vibrational assignments, keeping in minds that in argon like in nitrogen there could be also site splittings, enhancing spectral congestion (even if we did not encounter those typical spectral changes in the present study), but to go deeper into this identification, selective UV and IR irradiations are needed. At least, it should be noted that we did not observe a back isomerization toward $CCC_{OH/CO}$ by matrix annealing.

N_2 matrix. If UV broad band effects, displayed in Figure 6, are comparable to those observed in argon matrix, *i.e.* CCC species are isomerized toward nonchelated ones, vibrationnal assignment of those latters is more subtle because of the well-known trapping site multiplicity (especially we did not anneal the sample after irradiation). However, by analogy with argon matrix, after deposition there are only CCC isomers in nitrogen matrix. Following the same reasoning than in argon, we can confidently assign bands at 1650.0 and 1597.4 cm^{-1} ($\Delta\nu \approx 55.3$ cm^{-1} against 53.4 cm^{-1} theoretically, Table 2) to CCC_{CO} and those at 1641.7-1673.9-1641.7-1604.7-1602.8 and 1600.7 cm^{-1} ($\Delta\nu \approx 41.1$ cm^{-1} against 33.3 cm^{-1} theoretically, Table 2) to CCC_{OH}. After broad band UV irradiation, one observes $CCC_{OH/CO}$ bands decrease counterbalanced by the increase of those nonchelated. In the ν_{OH} region a broad HF-MF multiplet ranging between 3638 and 3598 cm^{-1} and a LF one between 3590 and 3568 cm^{-1}, grow. Both multiplets present the same shape, a high frequency side with a discrete structure while the low frequency part presents a kind of broad unstructured foot. Unlike in argon, one observes nonchelated consumption from 25 min of irradiation (against from 60 min in argon), but one observes also site exchanges rendering unambiguous vibrationnal assignments more difficult. Nevertheless, keeping in minds that excepted CCT_{CO}, CTC_{CO} and CTT_{CO}, it is the XXX_{OH} species that are likely to interconvert, we can suggest some identifications. So, after 25 min irradiation, one observes one LF decrease at 3580.9 cm^{-1} while two LF bands increase at 3585.8 and 3583.5 cm^{-1}, and, two HF decreases at 3629.1 and 3624.9 cm^{-1} against five increases at 3633.9, 3632.9, 3631.0, 3628.3, 3627.1 and 3623.1 cm^{-1}. Concomitantly in the $\nu_{C=O/C=C}$ region one observes decrease of the multiplets at 1715.0-1711.0-1708.2 and 1619.6-1618.1-1616.8 (*i.e* $\Delta\nu \approx 93$ cm^{-1}) and of one band centered at 1635.7 cm^{-1}(*i.e* $\Delta\nu \approx 76$ cm^{-1}). We also observe increases of multiplets peaked at 1685.5 and 1672.9 cm^{-1} (*i.e* $\Delta\nu \approx 13$ cm^{-1}). Considering this last $\Delta\nu$ is typical of TTT_{CO} and TCT_{CO} species (Table 2) coupled to the observation of HF increases at 3633.9, 3632.9 and 3631.0 cm^{-1}, *i.e.* the most "blue" ones, also compatible with these two species, we can assign those signals to them. As for the two HF decreasing bands at 3629.1 and 3624.9 cm^{-1}

coupled to the observation of the decrease at 1715.0 cm^{-1}, they only can be associated with CTT_{CO} isomer. Concerning the LF assignments, by analogy with argon matrix the 3580.9 cm^{-1} decreasing band, being the most "red" of the LF ones could be assigned to TCC_{OH} especially since we observe weak decreases at 1691.7 cm^{-1}, in the neighborhood of the one we assigned to this isomer in argon (1695.5 cm^{-1}, Table 2). However, in this last region, one observes other decreasing band $\Delta\nu$ of $\approx$ 93 cm^{-1}, what is only compatible with CXX species. There is unfortunetly no decisive help from the other spectral regions, we are thus led to tentatively suggest two options: considering the $\nu_{C=O/C=C}$ $\Delta\nu$, and the fact decreasing bands are surrounding the other nonchelated ones, it is impossible to discard the presence of CTC_{CO} and/or CTC_{OH} isomers but the decrease of their ν_{OH} bands could be hidden by the increases. At the same time, seeing no CXX increases, it means that the 3585.8 and 3583 cm^{-1} bands are due to TXX isomers. Since, in HF region we identified the decrease of CTT_{CO}, and that the 3580.9 cm^{-1} is potentially that of TCC_{OH}, we could assign 3585.8 and 3583.5 cm^{-1} bands to TCC_{CO}, TTC_{OH} or TTC_{OH}, or to two sites of the same isomer.

Ne matrix. In this matrix, which is the softest among the four we used, we observe the same scenario, *i.e.* upon UV broad band irradiation, $CCC_{OH/CO}$ isomers isomerize toward nonchelated ones (Figure 6). As in the two former matrices, bands at 1653.3 and 1597.7 cm^{-1} ($\Delta\nu \approx$ 55.6 cm^{-1} against 53.4 cm^{-1} theoretically, Table 2) are assigned to CCC_{CO} and those at 1647.9-1643.7 and the broad one at 1609.9 cm^{-1} ($\Delta\nu \approx$ 35.1 cm^{-1} against 33.3 cm^{-1} theoretically, Table 2) to CCC_{OH}. Upon broad band UV irradiation one observes grows, in the ν_{OH} region, of weak and broad HF-MF bands centered at 3678.9, 3670.9, 3655.6 cm^{-1} and of a LF multiplet ranging between 3630 and 3610 cm^{-1} with two maxima at 3623.0 and 3619.7 cm^{-1}. In the $\nu_{C=O/C=C}$ region, one observes the grow of bands roughly centered at 1717.0, 1700.0, 1697.0, 1694.2, 1690.5, 1686.1, 1678.4, 1668.9, 1642.1, 1640.2, 1634.9, 1626.7-1625.3 and 1618.0 cm^{-1}. A closer look to these bands reveal they exhibit more complex structures. The fact is also that neon matrix contains water pollution which allows us to discard, for

example, the band at 1630.7 cm^{-1} as possible AAD isomer candidate. It is a water polymer band.[38] As in the other matrices, one observes nonchelated band decreases after 45 min irradiation (Figure 6), *i.e.* isomerizations among nonchelated species. In the ν_{OH} region the most clear decrease is observed at 3617.9 cm^{-1}, *i.e.* the red foot of LF multiplet. By analogy with Ar and N_2 matrices, we assign this band to TCC_{OH}. This decrease is correlated to decrease at 1702.0 cm^{-1} in the $\nu_{C=O/C=C}$ region. By analogy with Ar matrix we also suggest to assign the decreasing band at 1699.6 cm^{-1} to TTT_{OH}. In the ν_{OH} region, after 45 min irradiation, one observes weak increases in the LF bands at 3622.4 cm^{-1}, and at 3678.5 and 3670.7 cm^{-1}, in the HF ones. At the same time, the only nonchelated bands (excepted those already assigned to TTT_{OH} and TCC_{OH}) we observe decreasing in the $\nu_{C=O/C=C}$ region at 1716.9, 1626.7-1625.3 and 1618.0 cm^{-1} are spaced by $\approx$ 92 and 100 cm^{-1} respectively, *i.e.* are typical of $CXX_{OH/CO}$ species. As a result, even we do not clearly observe $CXX_{OH/CO}$ ν_{OH} band decreases, the fact is that like in Ar matrix, those latter species are consumed. We suggest, by analogy with this former matrix, to assign the increasing LF band to TTC_{OH} (3622.4 cm^{-1}). Concerning the increasing HF and MF ones, at 3678.6, 3670.9 and 3655.6 cm^{-1}, even their intensities are really weak, they are already observable after 45 min irradiation, *i.e.* they are TXX, because CXX are consumed. By comparison with Ar matrix, and from Figure 4 and Table 2, we suggest to (tentatively) assign them to TCT_{CO} and TTT_{CO} (3685.7-3678.6 cm^{-1}), TCT_{OH} (3670.9 cm^{-1}) and TTT_{OH} (3655.6 cm^{-1}), respectively.

Xe matrix. As in the three other matrices, upon UV broad band irradiation one observes $CCC_{OH/CO}$ toward nonchelated species isomerization. To the contrary of what we observe in the former matrices, whether in ν_{OH} or $\nu_{C=O/C=C}$ region, spectra are more structured, bands are very sharp and then less in overlapping. Moreover, about 95 % of photochemical effect is achieved after only 5 min irradiation. Bands at 1643.9 and 1586.2 cm^{-1} ($\Delta\nu \approx 57.7$ cm^{-1} against 53.4 cm^{-1} theoretically, Table 2) should be associated with CCC_{CO} while those at 1636.6 and 1611.0-1601.0 cm^{-1} ($\Delta\nu \approx 25.6-35.6$ cm^{-1} against 33.3 cm^{-1} theoretically, Table

2) should be assigned to CCC_{OH}. In the ν_{OH} domain, grow of LF bands at 3581.4, 3578.6, 3574.6, 3569.4, 3566.9 and 3563.2 cm^{-1} is almost saturated after 5 min irradiation while those HF at 3612.9 and 3610.5 cm^{-1} grow during all the photochemical process. By observation of $\nu_{C=O/C=C}$ region, one observes again isomerization between nonchelated species from 25 min irradiation. In this last domain one observes main grows at 1704.8-1703.7, 1685.6, 1683.8, 1674.4, 1662.6, 1656.0-1654.7, 1639.0-1637.3, 1611.2, 1607.6 and 1586.2 cm^{-1}. The main decreases are at 1704.8 and 1611.2 cm^{-1} ($\Delta\nu \approx 93.6$ cm^{-1}), and 1607.6 cm^{-1} ($\Delta\nu \approx 97.2$ cm^{-1}). Those last $\Delta\nu$ are typical of CXX species, while the HF ν_{OH} increasing bands are typical of TXX ones. Decreases are also observed at 1683.8, 1655.8-1654.7 and 1639.0 cm^{-1}, and increases at 1685.6, 1674.4-1673.2 and 1662.4 cm^{-1} which are TXX species (with the exception of the 1639.0 cm^{-1} band which could be CTT_{OH} $\nu_{C=C}$ mode). Concomitantly, in the ν_{OH} region, one observes increases at 3612.9, 3610.5 and 3581.4 cm^{-1}. Considering that the only nonchelated species which could be consumed upon this UV irradiation are CTT_{CO} (HF, 221 nm), TCT_{OH} (HF, 231 nm), TTT_{OH} (MF, 231 nm), CTT_{OH} (MF, 232 nm), CTC_{OH} (LF, 230 nm) and TCC_{OH} (LF, 227 nm), we suggest to assign 3612.9, 1674.3 and 1662.6 cm^{-1} bands to TCT_{CO}, and 3610.5, 1673.2-1671.0 bands to TTT_{CO}. We also suggest to assign decreasing bands at 1683.8 and 1654.7 cm^{-1} bands to TTT_{OH}. The 1639.0 cm^{-1} band does not match a TXX one while it is located 28 cm^{-1} above CXX one at 1611.3 cm^{-1} . It could be associated with CTT_{OH}. The increasing bands at 3581.4 and 1685.6 cm^{-1} could only be associated with TTC_{OH}, because this is the only TXX isomer which presents a $\nu_{C=O}$ mode is this region, a LF ν_{OH} band and should not be consumed upon UV broad band irradiation (215 nm). Concerning the LF ν_{OH} decreasing bands at 3574.8, 3573.3, 3569.0, 3566.7 and 3563.2 cm^{-1} they can only be associated with CTC_{OH} and TCC_{OH}. Indeed, as mentioned above, they are the only LF species able to isomerize upon UV broad band irradiation. This fact, in the case of CTC_{OH}, is comforted by the observation of $\Delta\nu \approx 95$ cm^{-1} in the $\nu_{C=O/C=C}$ region.

Preliminary considerations on the electronic relaxation reactional pathway

In order to approach the electronic relaxation pathways, and based on our past experience with AA and MA (allowing us to take a critical look at this first set of results), we have carried out a first set of kinetics in all the matrices. As in the AA and MA cases,[1,2] the goal of such experiments is to observe a "heavy atom effect" on kinetic constants, or to observe a fragmentation, to inquire if AAD electronic relaxation processes through triplet state(s), like for AA, or singlet state(s), like for MA. It has been postulated that in AA case it is the *methyl-methyl* rotators coupling which induces the through triplet states electronic relaxation.[13] As can be seen from Figure 7, there is no clear heavy atom effect. Indeed, fitting experimental data with monoexponential functions, we found CCC_{XX} consumption kinetic constants ranging between 2.0 and 5.8 10^{-3} min^{-1}. The fact we do not observe a "heavy atom effect" could show that either a triplet state is not involved, or that the passage through T_1 state is very fast and is not a limiting step of the reaction pathways. Moreover, the isomerization rates being similar whatever the matrix indicates that reactional pathways are controlled mainly by intramolecular electronic and vibrational levels. However, in Ne and Xe matrices, one observes at the end of the UV photochemical process a weak fragmentation giving rise to weak but clear CO and fragments bands (those latter slightly blue shifted with respect to C=O, CTT_{XX} and CTC_{XX} bands). We certainly observe those fragments in Ne and Xe matrices because the former one is the softest matrix, allowing a better fragments diffusion, while the latter presents the largest cages. It demonstrates that, like AA, CCC_{XX} does not fragment, while, being not the main nonchelated species electronic relaxation result (because matrix cages prevent dissociation and induce more likely fast fragments recombination), nonchelated species fragment eventually in a triplet state. This kinetic study will be the subject of a forthcoming work.

Conclusion and Perspectives

In this work we have studied the broad band UV photochemistry of acetylacetaldehyde trapped in four cryogenic matrices, *i.e.* neon, argon, nitrogen and xenon. After deposition only two chelated species are observed while upon UV irradiation, they isomerize toward nonchelated isomers. Coupling this experimental work with theoretical calculations carried out at the TD-DFT ωB97XD/ 6-311++G(2d,2p) (UV transitions) and B3LYP/6-311G++(2d,2p) (potential minima and harmonic vibrational spectra) levels of theory, we have been able to identify several of them, the only ones never observed being CCT_{OH} and CCT_{CO}. Those latter isomers are the least stable because of strong $sp^2 - sp^3$ electronic lone pairs repulsion. Another goal of this work was also to compare AAD UV photochemistry with those of AA and MA. In a first approach, the study of AAD parent molecules consumption led to no clear "heavy atom effect", thus to no decisive clue to plead in favor of a through triplet state(s) electronic relaxation. However, in Ne and Xe matrices, at the end of UV photoprocess, *i.e.* close to the photoequilibrium, one observes nonchelated fragmentation and isomerization. Even fragments do not seem to be the main nonchelated photoproducts (partially because of the cage confinement leading to a fast fragments recombination), it could indicate, as in AA case, an electronic relaxation pathway through triplet(s) state. All these experiments should be repeated in presence of O_2 (in order to check if there is a triplet state quenching), and completed by IR and UV selective irradiations. If it is proved that AAD electronic relaxation proceeds through triplet state(s), it would mean that this is not the *methyl-methyl* coupling which induces a through triplet state(s) electronic relaxation, but uniquely the presence of one methyl substituent.

Table 1: Theoretical UV transitions calculated for the two first excited electronic states of each AAD isomers at the ωB97XD/6-311++G(2d,2p) level of theory (allowed transitions are written in bold characters).

Isomers	Transition	Wavelenght (eV)	Wavelenght (nm)	Oscillator strenghts
CCC_{CO}	$S_1 \leftarrow S_0/\pi^* \leftarrow n$	4.1275	300	0.0006
	$S_2 \leftarrow S_0/\pi^* \leftarrow \pi$	5.1356	**241**	0.2353
CCC_{OH}	$S_1 \leftarrow S_0/\pi^* \leftarrow n$	4.0280	308	0.0009
	$S_2 \leftarrow S_0/\pi^* \leftarrow \pi$	5.0066	**248**	0.2717
CCT_{CO}	$S_1 \leftarrow S_0/\pi^* \leftarrow n$	3.8909	319	0.0003
	$S_2 \leftarrow S_0/\pi^* \leftarrow \pi$	5.6969	**218**	0.3390
CCT_{OH}	$S_1 \leftarrow S_0/\pi^* \leftarrow n$	3.7335	332	0.0006
	$S_2 \leftarrow S_0/\pi^* \leftarrow \pi$	5.4595	**227**	0.3829
CTC_{CO}	$S_1 \leftarrow S_0/\pi^* \leftarrow n$	4.1344	300	0.0001
	$S_2 \leftarrow S_0/\pi^* \leftarrow \pi$	5.6561	**219**	0.3315
CTC_{OH}	$S_1 \leftarrow S_0/\pi^* \leftarrow n$	3.9257	316	0.0006
	$S_2 \leftarrow S_0/\pi^* \leftarrow \pi$	5.3902	**230**	0.3528
CTT_{CO}	$S_1 \leftarrow S_0/\pi^* \leftarrow n$	4.1178	301	0.0001
	$S_2 \leftarrow S_0/\pi^* \leftarrow \pi$	5.5999	**221**	0.3293
CTT_{OH}	$S_1 \leftarrow S_0/\pi^* \leftarrow n$	3.9075	317	0.0005
	$S_2 \leftarrow S_0/\pi^* \leftarrow \pi$	5.3392	**232**	0.3551
TCC_{CO}	$S_1 \leftarrow S_0/\pi^* \leftarrow n$	4.1554	298	0.0002
	$S_2 \leftarrow S_0/\pi^* \leftarrow \pi$	5.7360	**216**	0.3489
TCC_{OH}	$S_1 \leftarrow S_0/\pi^* \leftarrow n$	4.0061	309	0.0005
	$S_2 \leftarrow S_0/\pi^* \leftarrow \pi$	5.4518	**227**	0.4013
TCT_{CO}	$S_1 \leftarrow S_0/\pi^* \leftarrow n$	4.0700	310	0.0002
	$S_2 \leftarrow S_0/\pi^* \leftarrow \pi$	5.8784	**211**	0.3756
TCT_{OH}	$S_1 \leftarrow S_0/\pi^* \leftarrow n$	3.8900	319	0.0004
	$S_2 \leftarrow S_0/\pi^* \leftarrow \pi$	5.6012	**221**	0.4589
TTC_{CO}	$S_1 \leftarrow S_0/\pi^* \leftarrow n$	4.1763	297	0.0002
	$S_2 \leftarrow S_0/\pi^* \leftarrow \pi$	5.9195	**209**	0.4142
TTC_{OH}	$S_1 \leftarrow S_0/\pi^* \leftarrow n$	4.0964	303	0.0003
	$S_2 \leftarrow S_0/\pi^* \leftarrow \pi$	5.7732	**215**	0.4823
TTT_{CO}	$S_1 \leftarrow S_0/\pi^* \leftarrow n$	4.1365	300	0.0002
	$S_2 \leftarrow S_0/\pi^* \leftarrow \pi$	5.8749	**211**	0.4191
TTT_{OH}	$S_1 \leftarrow S_0/\pi^* \leftarrow n$	3.8033	326	0.0002
	$S_2 \leftarrow S_0/\pi^* \leftarrow \pi$	5.3777	**231**	0.1514

Table 2: Theoretical IR frequencies (not scaled) of all AAD isomers calculated B3LYP/6-311++G(2d,2p) level of calculation. Frequencies are given in cm^{-1}. Intensities are given in parenthesis and normalized to $\nu_{C=C}$ mode of CTC_{OH}.

Isomers[1]	ν_{OH}[2]	$\nu_{C=O}$	$\nu_{C=C}$	$\Delta\nu$[3]
CCC_{OH}	3218.3(*0.0*)	1646.2(*0.6*)[4]	1679.5(*0.4*)[5]	33.3
CCC_{CO}	3215.1(*0.0*)	1630.0(*0.3*)[4]	1683.4(*0.5*)[5]	53.4
TTT_{OH}	3827.4(*0.1*), MF	1729.4(*0.6*)	1700.9(*0.4*)	28.5
TTT_{CO}	3854.8(*0.2*), HF	1718.5(*0.3*)	1709.3(*0.5*)	9.2
TTC_{OH}	3797.5(*0.1*), LF	1728.4(*0.5*)	1673.2(*0.6*)	55.2
TTC_{CO}	3793.8(*0.1*), LF	1718.4(*0.4*)	1679.3(*0.6*)	39.1
TCC_{OH}	3791.8(*0.1*), LF	1735.2(*0.6*)	1671.3(*0.5*)	63.9
TCC_{CO}	3800.1(*0.1*), LF	1717.3(*0.4*)	1662.7(*0.5*)	54.6
TCT_{OH}	3840.3(*0.1*), HF	1729.7(*0.5*)	1705.3(*0.4*)	24.4
TCT_{CO}	3858.0(*0.2*), HF	1716.0(*0.3*)	1703.9(*0.3*)	12.1
CTT_{OH}	3821.1(*0.1*), MF	1748.3(*0.2*)	1653.7(*0.7*)	94.6
CTT_{CO}	3849.4(*0.2*), HF	1753.2(*0.3*)	1666.2(*0.6*)	87.0
CTC_{OH}	3795.1(*0.1*), LF	1746.9(*0.2*)	1630.5(*1.0*)	116.4
CTC_{CO}	3794.5(*0.1*), LF	1746.7(*0.3*)	1643.7(*0.9*)	103.0
CCT_{OH}	3821.8(*0.1*), MF	1761.6(*0.2*)	1665.5(*0.8*)	96.1
CCT_{CO}	3848.7(*0.2*), HF	1756.5(*0.3*)	1669.0(*0.4*)	87.5

[1] OH/CO underscripts indicate if methyl group is OH or CO side (see Figure S2).

[2] HF, MF, LF: High, Medium and Low Frequency, respectively.

[3] $\Delta\nu = |\nu_{C=O} - \nu_{C=C}|$.

[4] $\nu_{C=O}/\nu_{C=C}/\delta_{OH}$.

[5] $\nu_{C=C}/\nu_{C=O}$.

Table 3: Experimental IR frequencies of CCC_{OH} and CCC_{CO} in ν_{OH} and $\nu_{C=O/C=C}$ regions. Frequencies are given in cm^{-1}.

Vibrational modes	CCC_{OH}				CCC_{CO}			
	Ar	N_2	Ne	Xe	Ar	N_2	Ne	Xe
ν_{OH}	-	-	-	-	-	-	-	-
$\nu_{C=O}$	1608.2	1604.7	1609.9	1611.0	1594.3	1597.4	1597.7	1586.2
	1602.8	1602.8		1601.0	1591.1			
		1600.7						
$\nu_{C=C}$	1641.5	1645.1	1647.9	1636.6	1648.7	1650.0	1653.3	1643.9
		1643.9	1643.7		1647.0			
		1641.7						

Table 4: Experimental IR frequencies of CXX species in ν_{OH} and $\nu_{C=O/C=C}$ regions. Frequencies are given in cm^{-1}.

Vibrational modes	Tentative assignment	Ar	N_2	Ne	Xe
ν_{OH}	CTT_{OH}^{Ne}			3647.1	
	CTT_{OH}^{Ar}	3636.2			
	$CTT_{CO}^{N_2}$		3629.1		
	$CTT_{CO}^{N_2}$		3624.9		
			3623.1		
	$CTC_{OH}^{Ar}/CTC_{CO}^{Ar}$	3602.4			
					3578.6
					3574.6
					3569.4
					3566.9
					3563.2
$\nu_{C=O}$	CTT_{CO}^{Ne}			1719.8	
	$CTT_{OH}^{Ne}/CTC_{OH}^{Ne}/CTC_{CO}^{Ne}$			1716.9	
	$CTT_{CO}^{N_2}$		1715.0		
			1714.8		
			1712.4		
	CTT_{CO}^{Ar}	1712.2			
			1711.8		
			1711.0		
	CTT_{CO}^{Xe}				1708.8
			1708.2		
	$CTT_{OH}^{Ar}/CTC_{OH}^{Ar}/CTC_{CO}^{Ar}$	1707.8			
	$CTT_{OH}^{Xe}/CTC_{OH}^{Xe}/CTC_{CO}^{Xe}$				1704.8-1703.7
$\nu_{C=C}$	CTT_{OH}^{Xe}				1639.4
	CTC_{CO}^{Ne}			1626.7-1625.3	
		1621.1			
			1619.8		
			1618.1		
	CTC_{OH}^{Ne}			1618.0	
	CTC_{OH}^{Ar}	1616.9			
	CTC_{OH}^{Ar}	1615.3			
	CTC_{OH}^{Xe}				1612.4-1611.2
					1607.6
					1602.6

Table 5: Experimental IR frequencies of TXX species in ν_{OH} and $\nu_{C=O/C=C}$ regions. Frequencies are given in cm^{-1}. The most intense bands of a multiplet are underlined.

Vibrational modes	Tentative assignment	Ar	N_2	Ne	Xe
ν_{OH}	TCT_{CO}^{Ne}			3685.7	
	TTT_{CO}^{Ne}			3678.6	
	TCT_{OH}^{Ne}			3670.9	
	TTT_{OH}^{Ne}			3655.6	
		3649.8			
		3649.1			
	TTT_{OH}^{Ar}	3640.0			
	$TCT_{CO}^{N_2}$		3633.9		
	$TCT_{CO}^{N_2}$		3632.9		
	$TTT_{CO}^{N_2}$		3631.0		
			3628.3		
			3627.1		
	TTC_{OH}^{Ne}			3622.4	
			3619.7		
	TCC_{OH}^{Ne}			3617.9	
			3617.7		
					3613.0
	TCT_{CO}^{Xe}				3612.9
					3610.6
	TTT_{CO}^{Xe}				3610.5
		3600.2			
	TCC_{OH}^{Ar}	3597.3			

				3585.8	
				3583.5	
		TTC_{OH}^{Xe}			3581.4
		$TCC_{OH}^{N_2}$		3580.9	
					3578.6
					3574.6
					3569.4
					3566.9
					3563.2
$\nu_{C=O}$		TCC_{OH}^{Ne}		1702.0	
				1700.6	
		TTT_{OH}^{Ne}		1699.6	
		$TCT_{OH}^{Ne}/TTC_{OH}^{Ne}$		1697.5	
				1696.5	
				1695.5	
				1694.5	
				1690.6	
		TCC_{OH}^{Ar}	1695.5		
		$TCC_{OH}^{N_2}$		1691.7	
		TTT_{OH}^{Ar}	1691.5		
				1690.2	
		$TCT_{OH}^{Ar}/TTC_{OH}^{Ar}$	1689.3		
				1688.9	
		$TCT_{OH}^{Ar}/TTC_{OH}^{Ar}$	1688.6		
				1688.2	
				1686.9	
		$TCT_{OH}^{Ar}/TTC_{OH}^{Ar}$	1686.6		

	$TTT_{CO}^{Ne}/TCT_{CO}^{Ne}/TTC_{CO}^{Ne}$			1686.4	
	TTC_{OH}^{Xe}				1685.6
			1685.5		
			1684.1		
	TTT_{OH}^{Xe}				1683.8
	$TTT_{CO}^{Ar}/TCT_{CO}^{Ar}/TTC_{CO}^{Ar}/TCC_{CO}^{Ar}$	1676.8			
	$TTT_{CO}^{Ar}/TCT_{CO}^{Ar}/TTC_{CO}^{Ar}/TCC_{CO}^{Ar}$	1675.0			
	TCT_{CO}^{Xe}				1674.3
			1674.0		
	TTT_{CO}^{Xe}				1673.2-1671.0
			1672.9		
$\nu_{C=C}$	TTT_{CO}^{Ne}			1678.3	
	TTT_{OH}^{Ne}			1668.9	
	$TTT_{CO}^{Ar}/TCT_{CO}^{Ar}/TCT_{OH}^{Ar}$	1667.7			
	$TTT_{CO}^{Ar}/TCT_{CO}^{Ar}/TCT_{OH}^{Ar}$	1666.3			
	TCT_{CO}^{Xe}				1662.6
	TTT_{OH}^{Xe}				1654.7
	TCC_{OH}^{Ne}			1641.8	
	TTC_{OH}^{Ne}			1640.4	
	$TTC_{CO}^{Ar}/TTC_{OH}^{Ar}$	1640.0			
	$TTC_{CO}^{Ar}/TTC_{OH}^{Ar}$	1638.4			

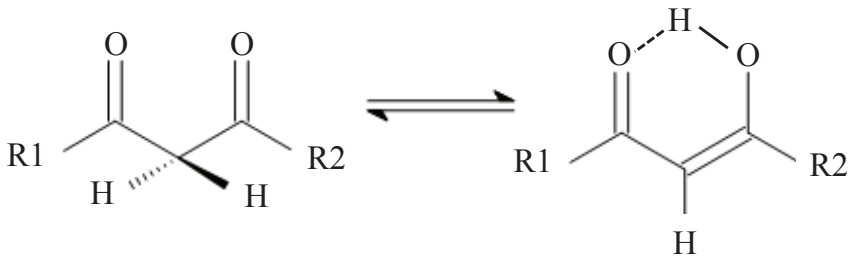

Keto Enol

R1 : H or CH_3
R2 : H or CH_3

Figure 1: Keto-Enol equilibrium of malonaldehyde, acetylacetone and acetylacetaldehyde ($R1 = H, R2 = CH_3$, and *vice-versa*).

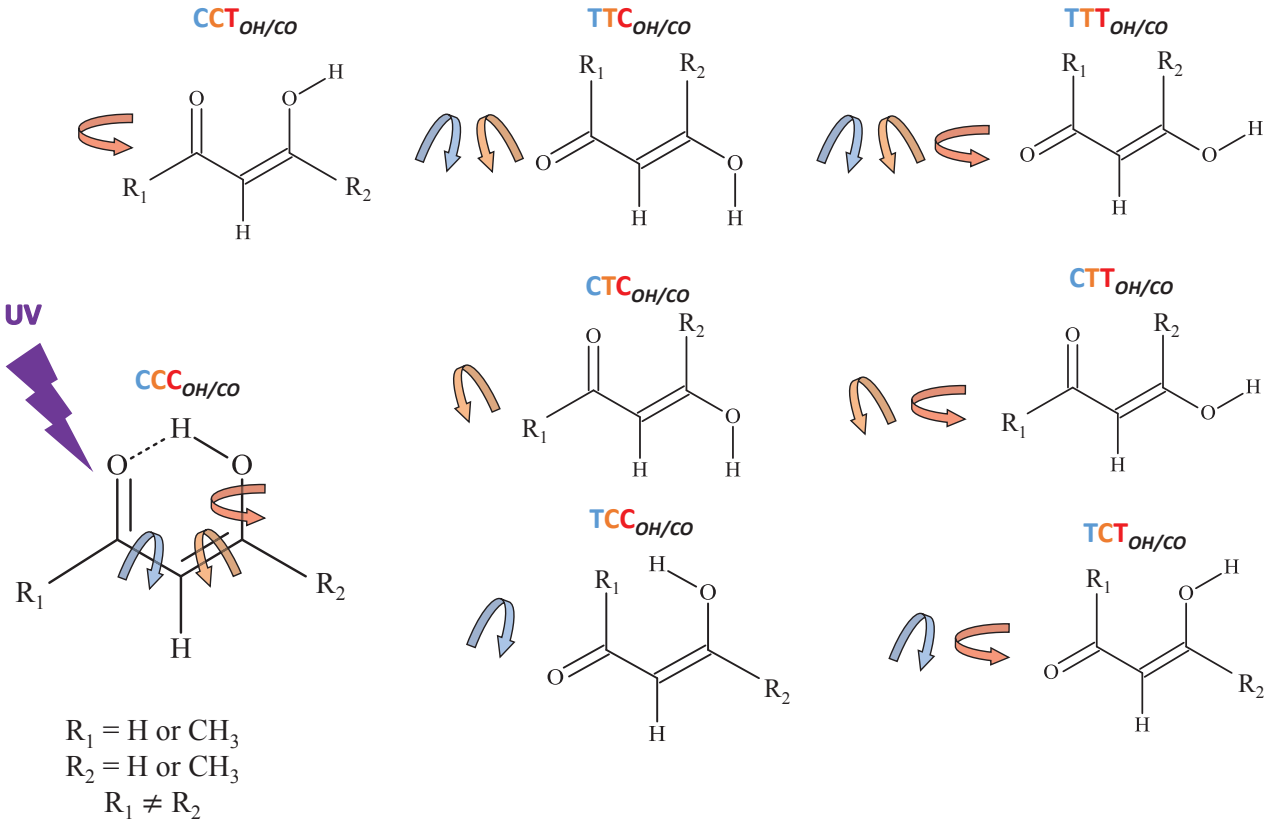

Figure 2: Picture of all AAD isomers. Non-chelated forms are obtained by UV irradiation of CCC, only form present after deposition. C and T stand for *Cis* and *Trans* characters relative to C-C, C=C and C-O bonds. OH and CO underscripts stand for the "side" methyl group is attached, or C=O or O-H one. For relative energies obtained at the B3LYP/6-311G++(2d,2p) level of theory, see Table 2.

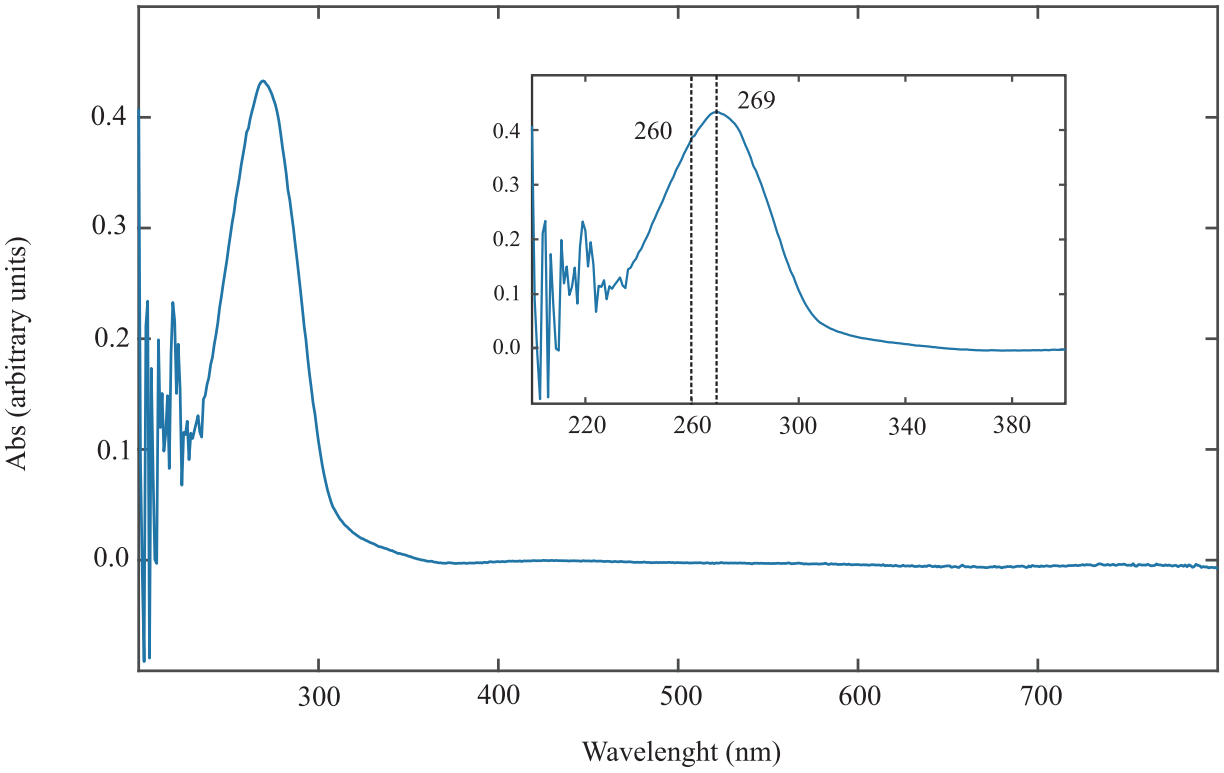

Figure 3: UV spectrum of AAD diluted in dichloromethane at 298 K.

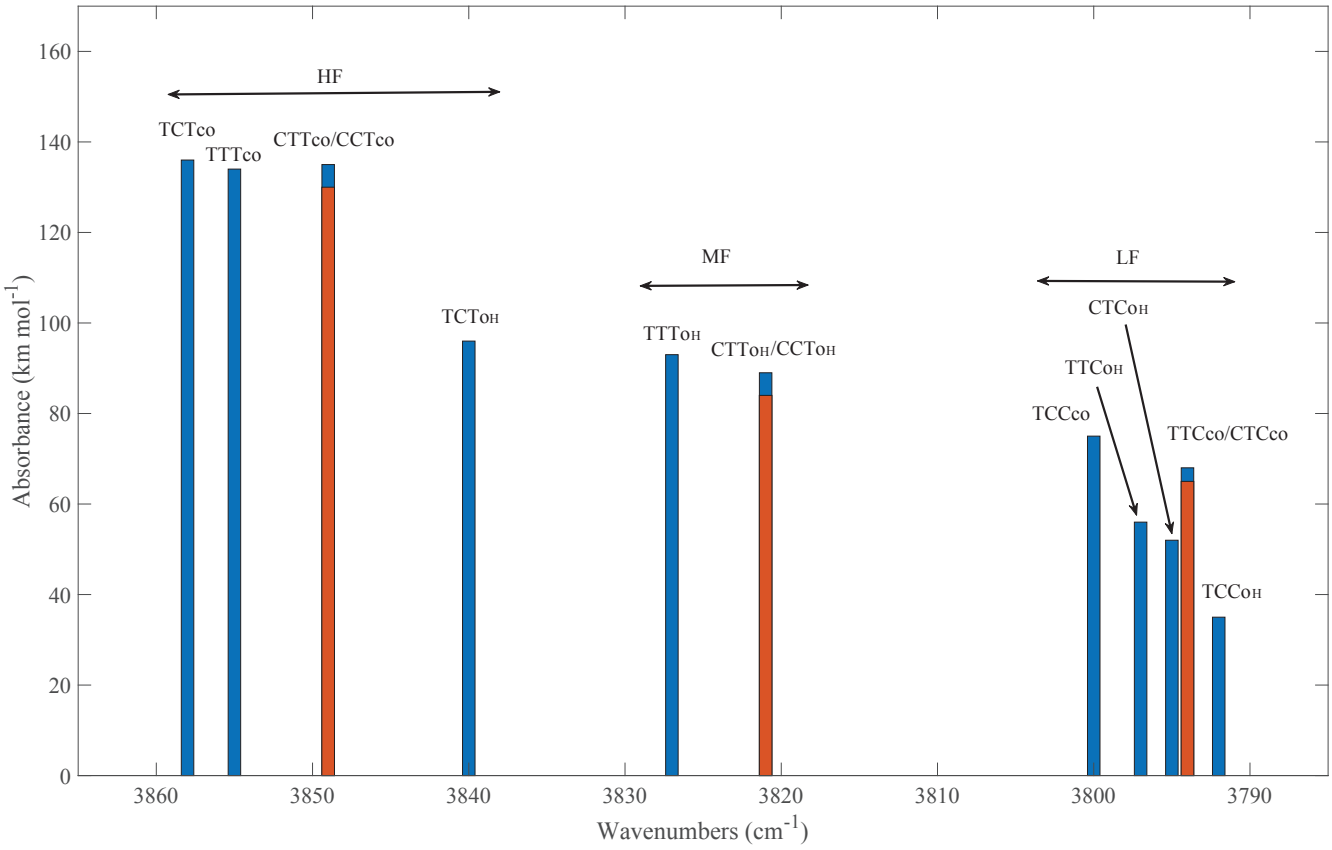

Figure 4: ν_{OH} (3860-3790 cm^{-1}) modes of all nonchelated AAD isomers calculated at the B3LYP/6-311G++(2d,2p) level of calculation. HF, MF and LF stand for High, Medium and Low Frequencies, respectively. The three red bands correspond to overlapping between CTT_{CO} and CCT_{CO} at 3849 cm^{-1}, those of CTT_{OH} and CCT_{OH} at 3821 cm^{-1}, and those of TTC_{CO} and CTC_{CO} at 3794 cm^{-1}.

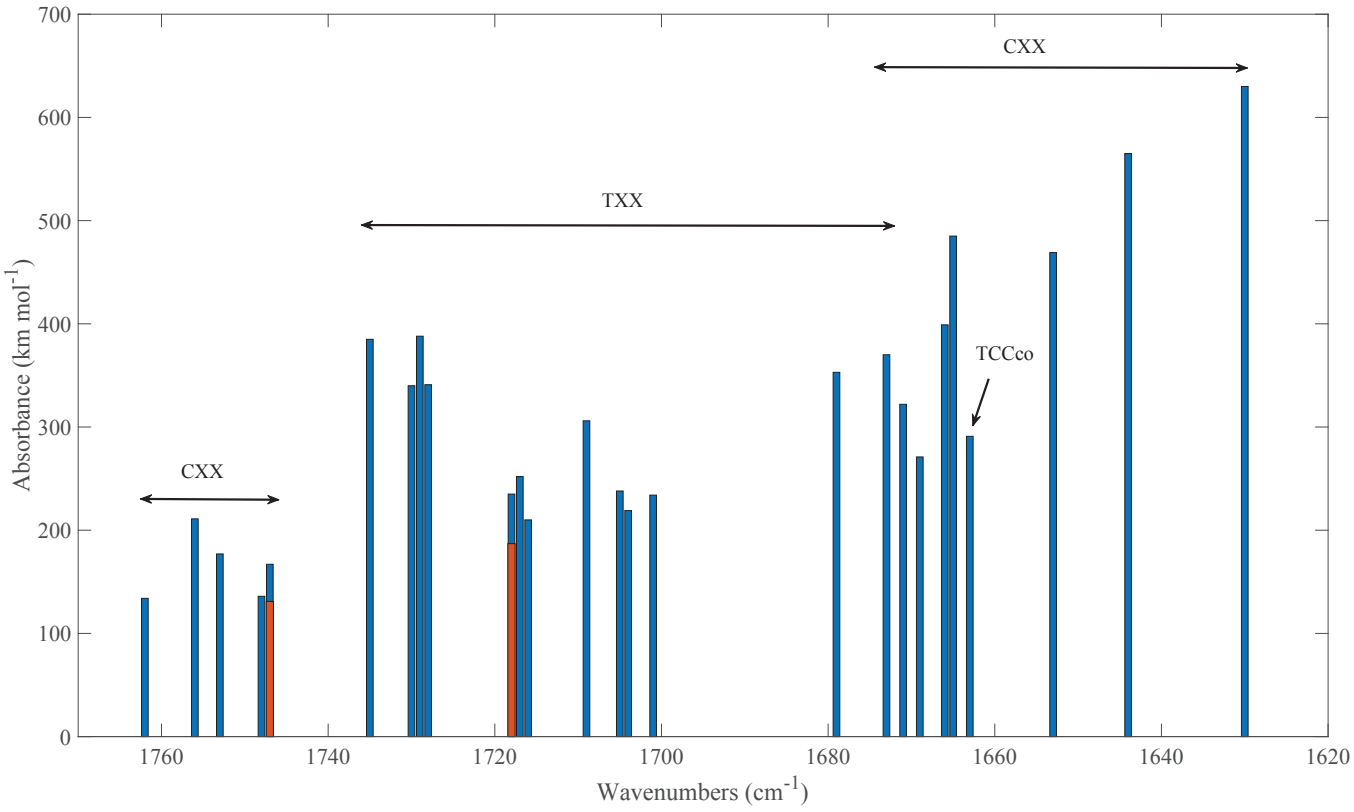

Figure 5: $\nu_{C=O}$ (1742-1718 cm^{-1}) and $\nu_{C=C}$ (1709-1630 cm^{-1}) modes of all nonchelated AAD isomers calculated at the B3LYP/6-311G++(2d,2p) level of calculation. The CXX species $\Delta\nu$ ($\Delta\nu = |\nu_{C=O} - \nu_{C=C}|$) range between 117 and 87 cm^{-1} against 64 and 9 cm^{-1} for TXX species. The two red bands correspond to overlapping between CTC_{OH} and CTC_{CO} $\nu_{C=O}$ modes at 1747 cm^{-1}, and those of TTC_{CO} and TTT_{CO} at 1718 cm^{-1}.

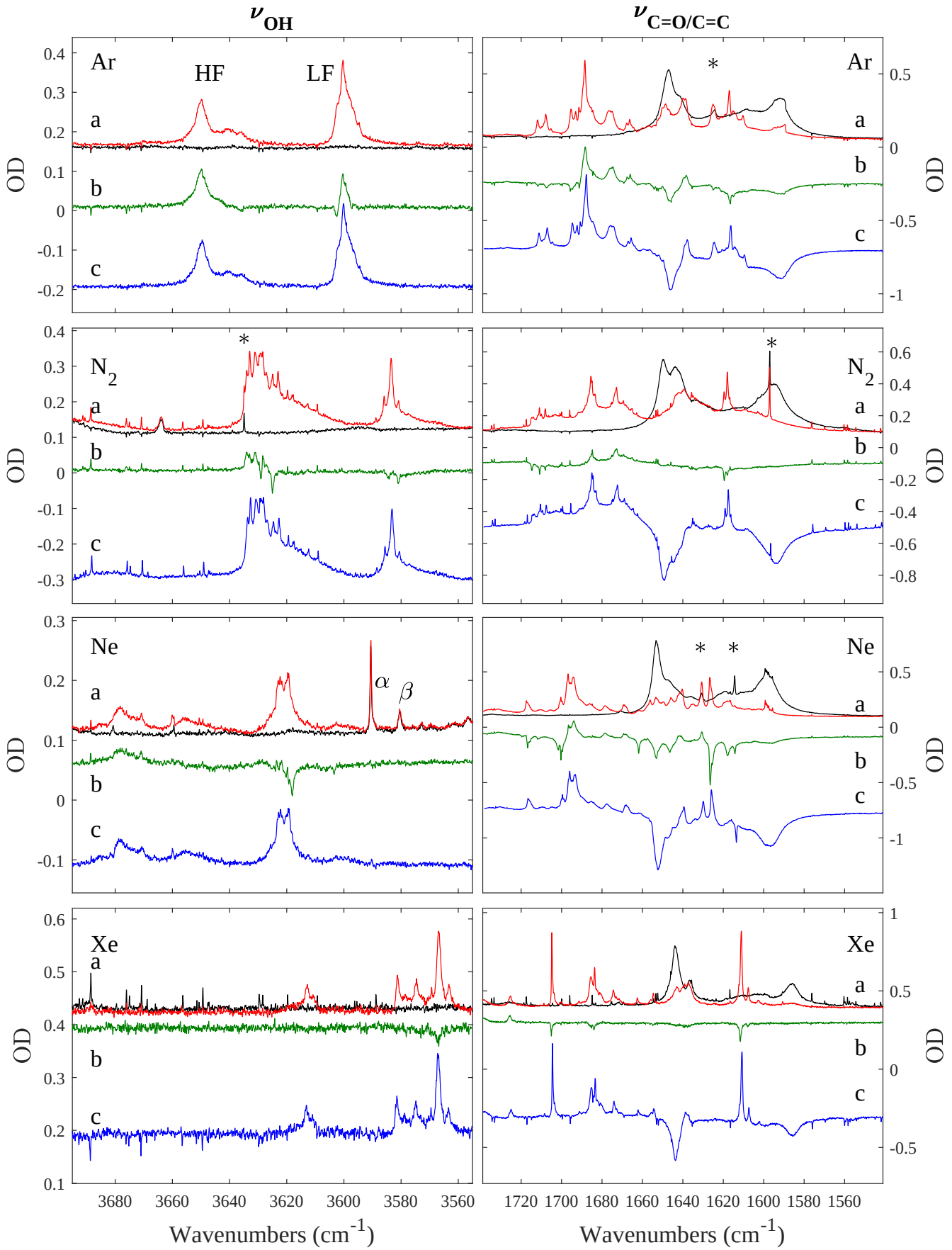

Figure 6: (Caption on next page.)

Figure 6: (Previous page.) Broad band UV irradiation (lamp power, 300 W) of acetylacetaldehyde trapped at 3.8 K, in Ar, N_2, Ne, and Xe. In Ar: (a) black spectrum, after deposition; red spectrum, after 500 min irradiation; (b): difference spectrum (after 500 min irradiation - after 60 min irradiation); (c): difference spectrum (after 500 min irradiation - after deposition). In N_2: (a) black spectrum, after deposition; red spectrum, after 115 min irradiation; (b): difference spectrum (after 115 min irradiation - after 25 min irradiation); (c): difference spectrum (after 115 min irradiation - after deposition). In Ne: (a) black spectrum, after deposition; red spectrum, after 335 min irradiation; (b): difference spectrum (after 335 min irradiation - after 45 min irradiation); (c): difference spectrum (after 335 min irradiation - after deposition). α and β water dimers proton donors. In Xe : (a) black spectrum, after deposition; red spectrum, after 125 min irradiation; (b): difference spectrum (after 125 min irradiation - after 25 min irradiation); (c): difference spectrum (after 125 min irradiation - after deposition). α and β, in Ne, are two proton donor partners of water dimers. $*$ refers to water traces.

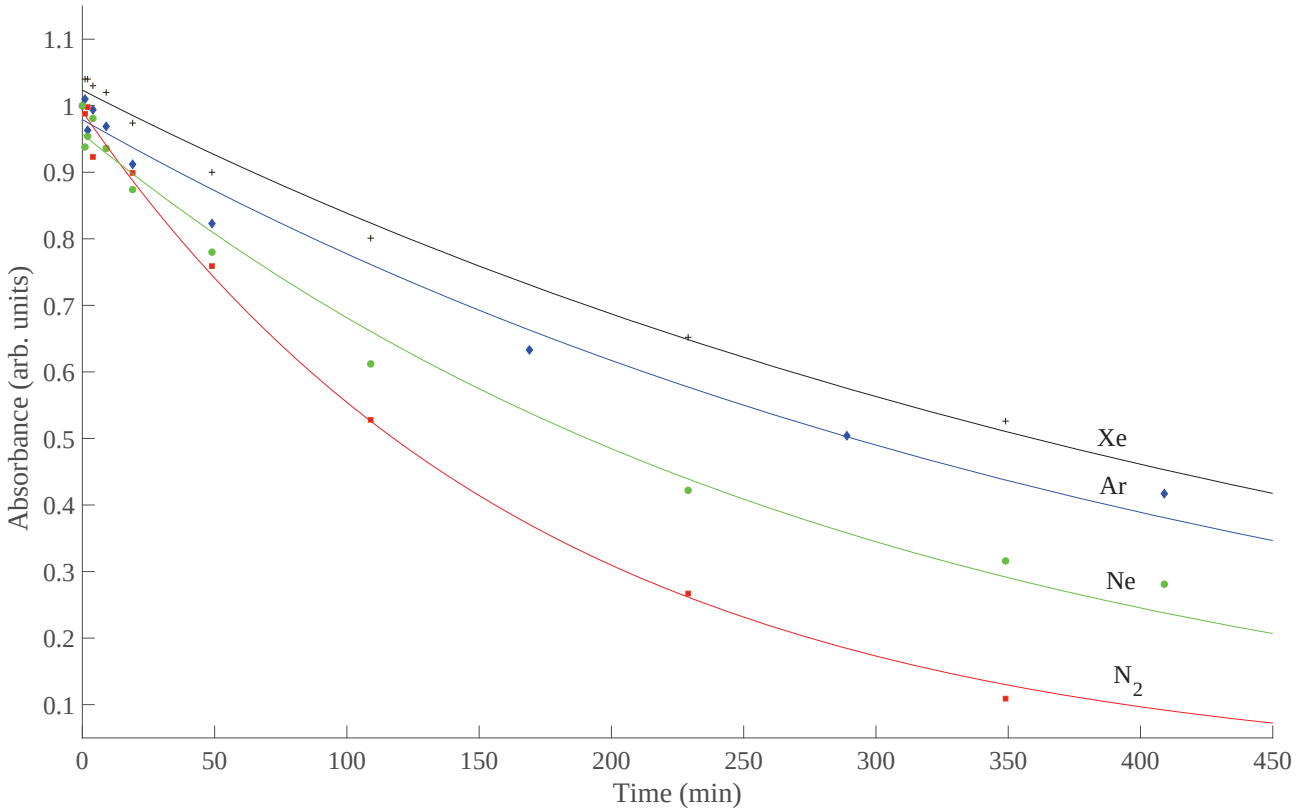

Figure 7: Kinetics of CCC_{XX} consumption upon broad band UV irradiation (lamp power, 100 W, no water filter) of acetylacetaldehyde trapped at 3.8 K, in Ar, N_2, Ne, and Xe. Integration ranges and kinetic constants are, in Ar: 1488-1453 cm^{-1}, $k_{Ar} = 2.3\ 10^{-3}$ min^{-1}; in N_2: 1470-1450 cm^{-1}, $k_{N_2} = 5.8\ 10^{-3}$ min^{-1}; in Ne: 1476-1452 cm^{-1}, $k_{Ne} = 3.4\ 10^{-3}$ min^{-1} and in Xe: 1476-1444 cm^{-1}, $k_{Xe} = 2.0\ 10^{-3}$ min^{-1};

References

(1) Trivella, A.; Wassermann, T. N.; Manca Tanner, C; Lüttschwager, N. O. B.; Coussan, S. UV and IR Photochemistries of Malonaldehyde Trapped in Cryogenic Matrices. *J. Phys. Chem. A*, **2018**, *122*, 2376-2393.

(2) Trivella, A.; Wassermann, T. N.; Mestdagh, J.M.; Manca Tanner, C; Marinelli, F; Roubin, P.; Coussan, S. New Insights into the Photodynamics of Acetylacetone: Isomerization and Fragmentation in Low-Temperatures Matrixes. *PCCP*, **2010**, *12*, 8300-8312.

(3) Coussan, S.; Ferro, Y; Trivella, A.; Rajzmann, M.; Roubin, P.; Wieczorek, R.; Manca, C., Piecuch, P.; Kowalski, K,; Wloch, M.; Kucharski, SA.; Musial, M. Experimental and Theoretical UV Characterizations of Acetylacetone and its Isomers. *J. Phys. Chem. A*, **2006**, *110*, 3920-3926.

(4) Trivella, A.; Coussan, S.; Chiavassa, T.; Theulé, P.; Roubin, P.; Coussan, S. Comparative Study of Structure and Photo-induced Reactivity of Malonaldehyde and Acetylacetone Isolated in Nitrogen Matrices. *Low Temperature Physics*, **2006**, *32*, 1042-1049.

(5) Wassermann, T. N.; Luckaus, D.; Coussan, S.; Suhm, M. A. Proton Tunneling Estimates for Malonaldehyde Vibrations from Supersonic Jet and Matrix Quenching Experiments. *PCCP*, **2006**, *8*, 2344-2348.

(6) Lüttschwager, N. O. B.; Wassermann, T. N.; Coussan, S.; Suhm, M. A. Periodic Bond Breaking and Making in Electronic Ground State on a Sub-picosecond Timescale: OH Bending Modes of Malonaldehyde at Low Temperature. *PCCP*, **2010**, *12*, 8201-8207.

(7) Lüttschwager, N. O. B.; Wassermann, T. N.; Coussan, S.; Suhm, M. A. Vibrational Tuning of the Hydrogen Transfer in Malonaldehyde-A Combined FTIR and Raman Jet Study. *Molecular Physics*, **2013**, *111*, 20-32.

(8) Dannenberg, J. J.; Rios, R. Theoretical Study of the Enolic Forms of Acetylacetone. How Strong is the Hydrogen Bond? *J. Phys. Chem*, **1994**, *98*, 6714-6718.

(9) Lozada-Garcia, R. R.; Ceponkus, J.; Wutharat, C.; Chevalier, M.; Crépin, C. Acetylacetone in Hydrogen Solids: IR Signatures of the Enol and Keto Tautomers and UV Induced Tautomerization. *Chem. Phys. Lett.*, **2011**, *504*, 142-147.

(10) Yoon, M. C.; Choi, Y. S.; Kim S. K. Photodissociation Dynamics of Acetylacetone: The OH Product State Distribution. *J. Chem. Phys.*, **1999**, *110*, 11850-11855.

(11) Upadhyaya, H. P.; Kumar, A.; Naik, P. D. Photodissociation Dynamics of Enolic-Acetylacetone at 266, 248 and 193 nm: Mechanism and Nascent State Product Distribution of OH. *J. Chem. Phys.*, **2003**, *118*, 2590-2598.

(12) Xu, S.; Park, S. T.; Feenstra, J. S.; Srinivisan, R.; Zewail A. H. Ultrafast Electron Diffraction: Structural Dynamics of the Elimination Reaction of Acetylacetone. *J. Phys. Chem. A*, **2004**, *108*, 6650-6655.

(13) Poisson, L.; Roubin, P.; Coussan, S.; Soep B.; Mestdagh, J-M. Ultrafast Dynamics of Acetylacetone (2,4-Pentanedione) in the S_2 State. *JACS*, **2008**, *130*, 2974-2983.

(14) Ríos, M. A.; Rodríguez, J. Analysis of the Effect of Substitution on the Intramolecular Hydrogen Bond of Malonaldehyde by Ab Initio Calculations at the 3-21G Level. *J. Mol. Struct. THEOCHEM*, **1991**, *228*, 149-158.

(15) Nowroozi, A.; Jalbout, A. F.; Roohi, H.; Khalilinia, E.; Sadeghi, M.; De Leon, A.; Raissi, H. Hydrogen Bonding in Acetylacetaldehyde: Theoretical Insights from the Theory of Atoms in Molecules. *Int. J. Quantum Chem.*, **2009**, *109*, 1505-1514.

(16) Chiavassa, T.; Verlaque, P.; Pizzala, L.; Roubin, P. Vibrational Studies of Methyl Derivatives of Malonaldehyde: Determination of a Reliable Force Field for β-dicarbonyl Compounds. *Spectrochimica Acta A*, **1993**, *50A*, 343-351.

(17) Bothner-By, A. A.; Harris, R. K.; Conformational Preferences in Malondialdehyde and Acetylacetaldehyde Enols Investigated by Nuclear Magnetic Resonance. *J. Organic Chem.*, **1965**, *30*, 254-257.

(18) George, W. O.; Mansell, V. G. Nuclear Magnetic Resonance Spectra of Acetylacetaldehyde and Malondialdehyde. *J. Chem. Society B: Physical Organic*, **1968**, 132-134.

(19) Zhao, D-X.; Zhao, J.; Song, M.; Zhu, Z-W.; Chen, C-C.; Song, Y-J. Changing Pictures of Molecular Faces and Depths of Potential Acting on an Electron in Molecule for Intramolecular Proton Transfer Reactions of Formic Acid and Malonaldehyde. *Computational and Theoretical Chemistry*, **2017**, *1115*, 88-98.

(20) Wu, F.; Ren, Y.; Bian, W. The Hydrogen Tunneling Splitting in Malonaldehyde: A Full-dimensional Time-dependant Quantum Mechanical Method. *J. Chem. Phys.*, **2016**, *15*, 074309/1-9.

(21) Wu, F.; Ren, Y. Primary and Secondary Isotope Effect on Tunneling in Malonaldehyde Using a Quantum Mechanical Scheme. *Molecular Physics*, **2017**, *115*, 1700-1707.

(22) Choi, C.; Pintar, M. Tunneling Splitting Due to Weak Coupling between Methyl Rotators in Acetylacetone. *J. Chem. Phys.*, **1997**, *106*, 3473-3476.

(23) Chen, X-B.; Fang, W-H.; Phillips D. L. Theoretical Studies of the Photochemical Dynamics of Acetylacetone: Isomerization, Dissociation, and Dehydration Reactions. *J. Phys. Chem. A*, **2006**, *110*, 4434-4441.

(24) Coe, J. D.; Martinez, T. J. Ab Initio Molecular Dynamics of Excited-State Intramolecular Proton Transfer around a Three-State Conical Intersection in Malonaldehyde. *J. Phys. Chem. A*, **2006**, *110*, 618-630.

(25) Coe, J. D.; Ong, M. T.; Levine, G.; Martinez, T. J. On the Extent and Connectivity

of Conical Intersection Seams and the Effects of Three-State Intersections. *J. Phys. Chem. A*, **2008**, *112*, 12559-12567.

(26) Chai, J-D.; Head-Gordon, M. Long-range Corrected Hybrid Density Functionals with Damped Atom-atom Dispersion Corrections. *PCCP*, **2008**, *10*, 6615-6620.

(27) Bloino, J.; Biczysko, M.; Santoro, F.; Barone, V. General Approach to Compute Vibrationally Resolved One-Photon Electronic Spectra. *JCTC*, **2010**, *6*, 1259-1274.

(28) Frisch, M. J. *et al* Gaussian16, Revision B.01, **2016**, Inc., Wallingford CT.

(29) Krishman, R.; Binkley, J. S.; Seeger, R.; Pople, J. A. Self-Consistent Molecular Orbitals Methods. XX. A Basis Set for Correlated Wavefunctions. *J. Chem. Phys.*, **1980**, *72*, 650-654.

(30) Frisch, M.; Pople, J. A.; Binkley, J. S. Self-Consistent Molecular Orbitals Methods 25. Supplementary Functions for Gaussian Basis Sets. *J. Chem. Phys.*, **1984**, *80*, 3265-3269.

(31) Becke, A. D. Density-Functional Thermochemistry. III. The Role of Exact Exchange. *J. Chem. Phys.*, **1993**, *98*, 5648-5652.

(32) Becke, A. D. Density-Functional Thermochemistry. 5. Systematic Optimization of Exchange-Correlation Functionals. *J. Chem. Phys.*, **1997**, *107*, 8554-8560.

(33) Lee, C.; Wang, W.; Parr, R. G. Development of the Cole-Salvetti Correlation-Energy Formula into a Functional of the Electron Density. *Phys. ReV. B*, **1988**, *37*, 785-789.

(34) Trivella, A.; Roubin, P.; Theulé, P.; Rajzmann, M.; Manca, C.; Coussan, S. UV and IR Photoisomerization of Acetylacetone in a Nitrogen Matrix. *J. Phys. Chem. A*, **2007**, *111*, 3074-3081.

(35) Baughcum, S. L.; Duerst, R. W.; Rowe, W. F.; Smith, Z.; Wilson E. B. Microwave Spectroscopic Study of Malonaldehyde (3-hydroxy-2-propenal.2. Structure, Dipole-Moment and Tunneling. *JACS*, **1981**, *103*, 6296-6303.

(36) Baba, T.; Tanaka, T.; Morino, I.; Yamada, K. M. T.; Tanaka, K. Detection of the Tunneling-Rotation Transitions of Malonaldehyde in the Submillimeter-wave region. *J. Chem. Phys.*, **1999**, *110*, 4131-4133.

(37) Bratos, S.; Ratajczak, H. Profiles of Hydrogen Stretching IR Bands of Molecules with Hydrogen Bonds: A Stochastic Theory. II. Strong Hydrogen Bonds *J. Chem. Phys.*, **1982**, *76*, 77-85.

(38) Coussan, S.; Roubin, P.; Perchard, J.P. Infrared Induced Isomerizations of Water Polymers trapped in Nitrogen Matrix *Chem. Phys.*, **2006**, *324*, 527-540.

Supplementary Material

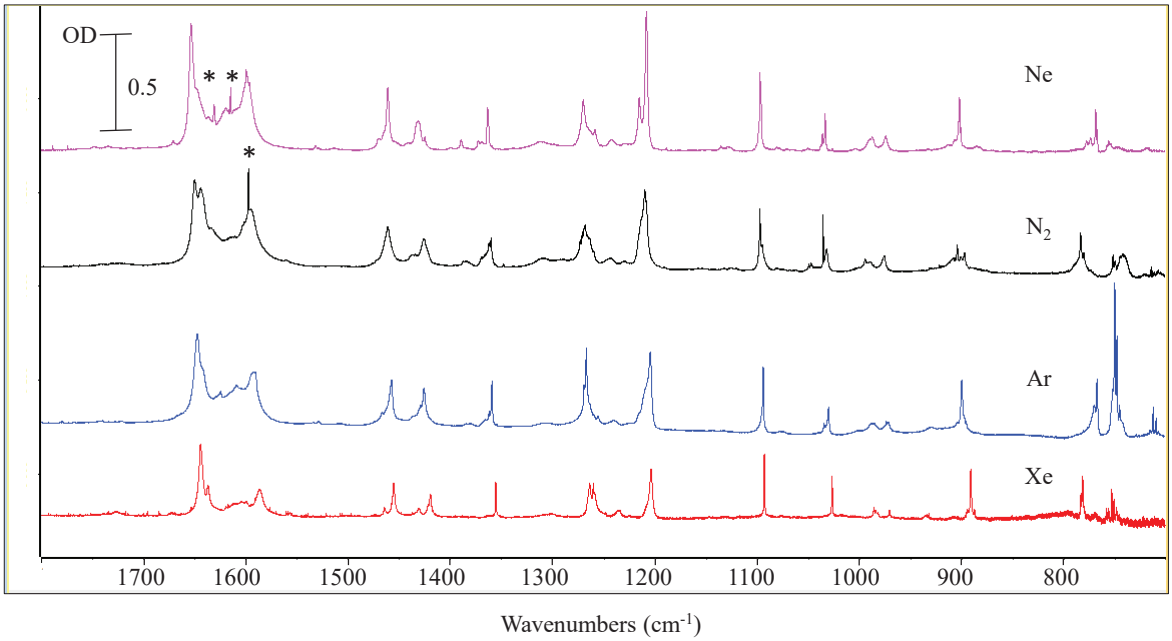

Figure S1: CCC_{XX} vibrational spectra in Ne, N_2, Ar and Xe matrices. Only the region ranging between 1800 and 700 cm^{-1} is shown because ν_{OH} modes are not observable (see text) and ν_{CH} region is composed of weak bands ranging between 3090 and 2650 cm^{-1}. *water traces.

Table S1: Experimental IR frequencies of CCC_{XX} species in 1500-700 cm^{-1} region. Frequencies are given in cm^{-1}. Only the most intense bands are reported.

Ne	N_2	Ar	Xe
1460.9	1460.9	1466.4	1463.6
1441.2	1437.6	1457.1	1454.8
1432.8	1425.7	1429.1	1430.1
1430.1	1361.6	1425.1	1418.9
1424.5	1359.5	1361.5	1354.9
1388.8	1267.7	1358.7	1263.2
1363.4	1212.8	1268.6	1258.6
1362.5	1209.2	1266.3	1202.9
1269.0	1207.6	1209.5	1092.3
1258.0	1096.8	1203.8	1026.0
1214.6	1094.1	1093.2	984.9
1207.5	1034.6	1033.8	982.9
1096.5	1031.6	1029.2	981.0
1095.3	1030.9	987.7	969.8
1035.2	993.5	984.4	889.8
1032.5	988.9	975.1	782.5
989.1	975.0	972.8	780.6
986.3	903.4	899.1	752.0
973.4	896.2	769.2	
901.2	782.7	766.4	
777.0	750.8	747.0	
772.9	748.9	744.6	
767.8	740.9		
755.2			

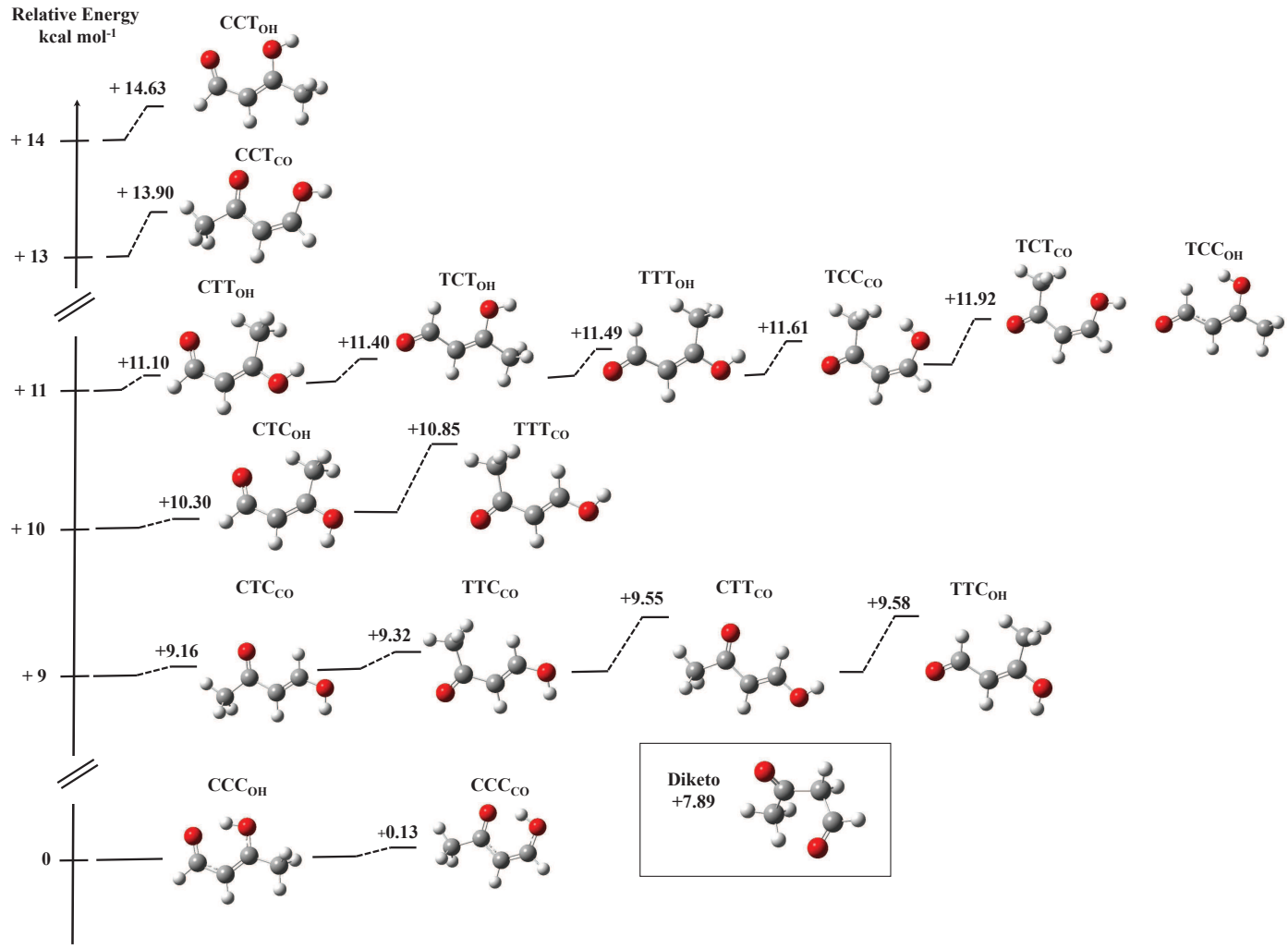

Figure S2: S_0 minima of AAD calculated at the B3LYP/6-311G++(2d,2p) level of calculation. Relatives energies (in kcal mol^{-1}) are given with respect to CCC_{OH}. Scale is not respected.

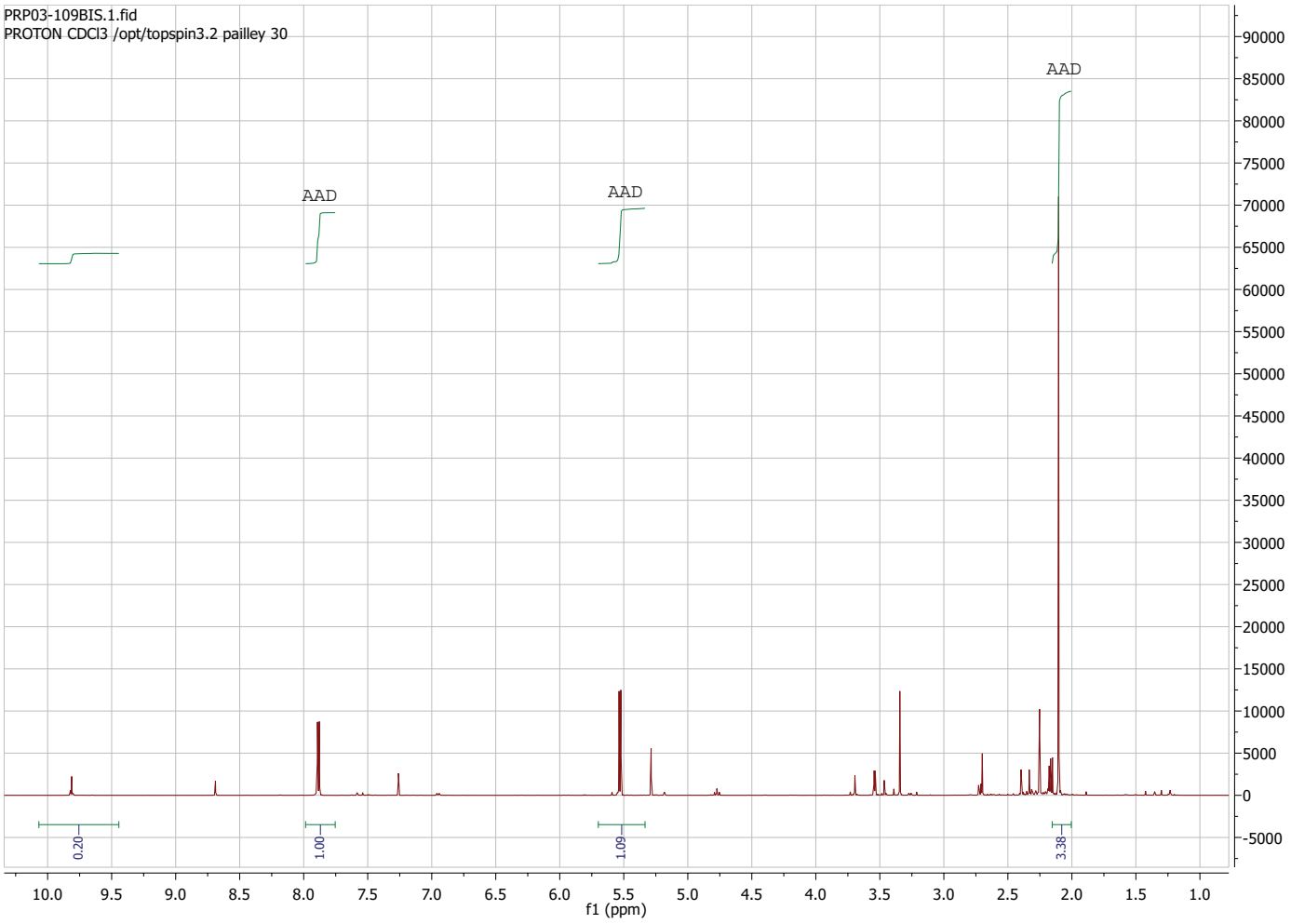

Figure S3: ^{1}H NMR spectrum of Acetylacetaldehyde in $CDCl_3$. Multiplets at 2.1, 5.55 and 7.9 ppm are typical of AAD.

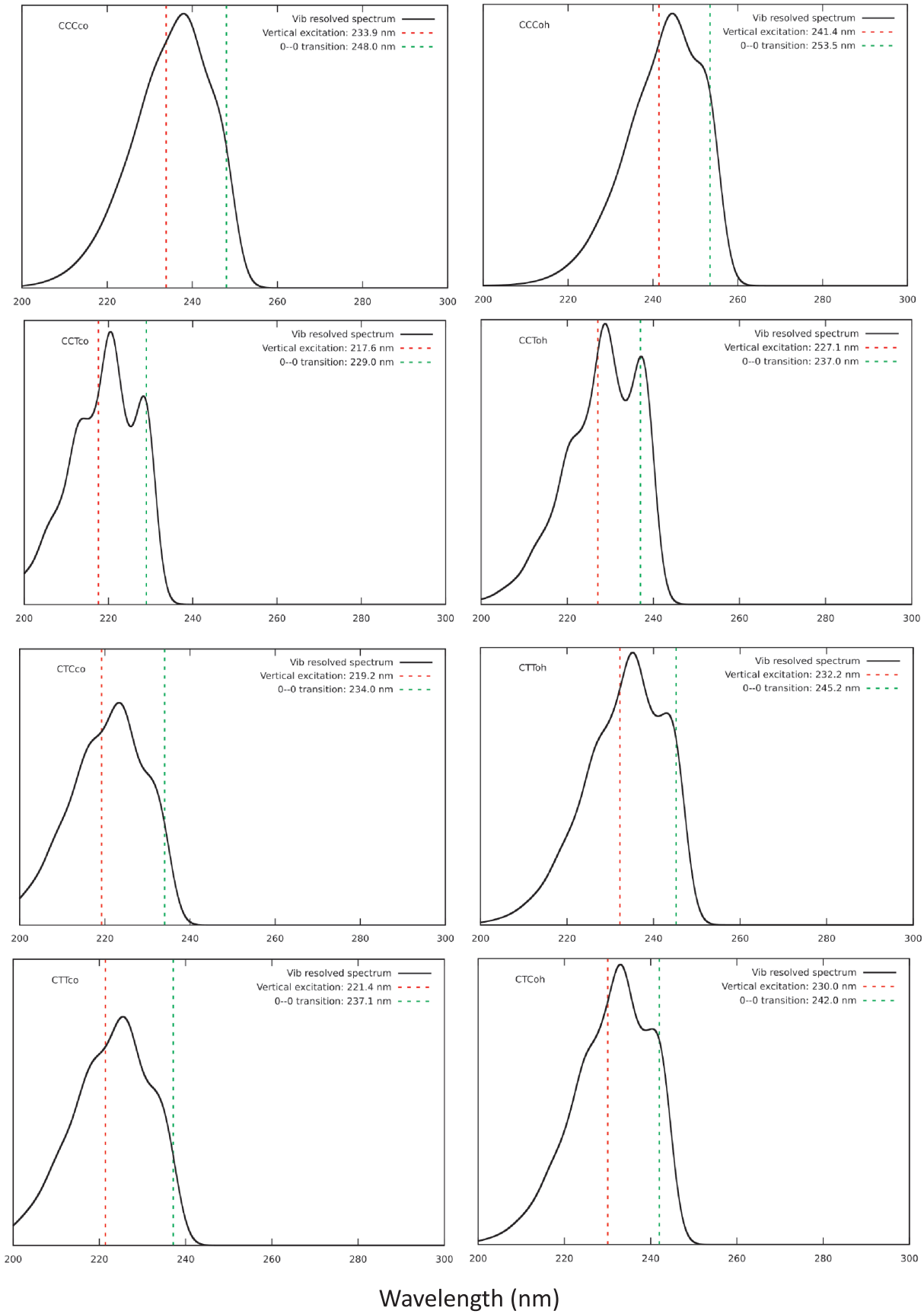

Figure S4: Theoretical UV absorption spectra of CXXxx species (for calculation details, see text)

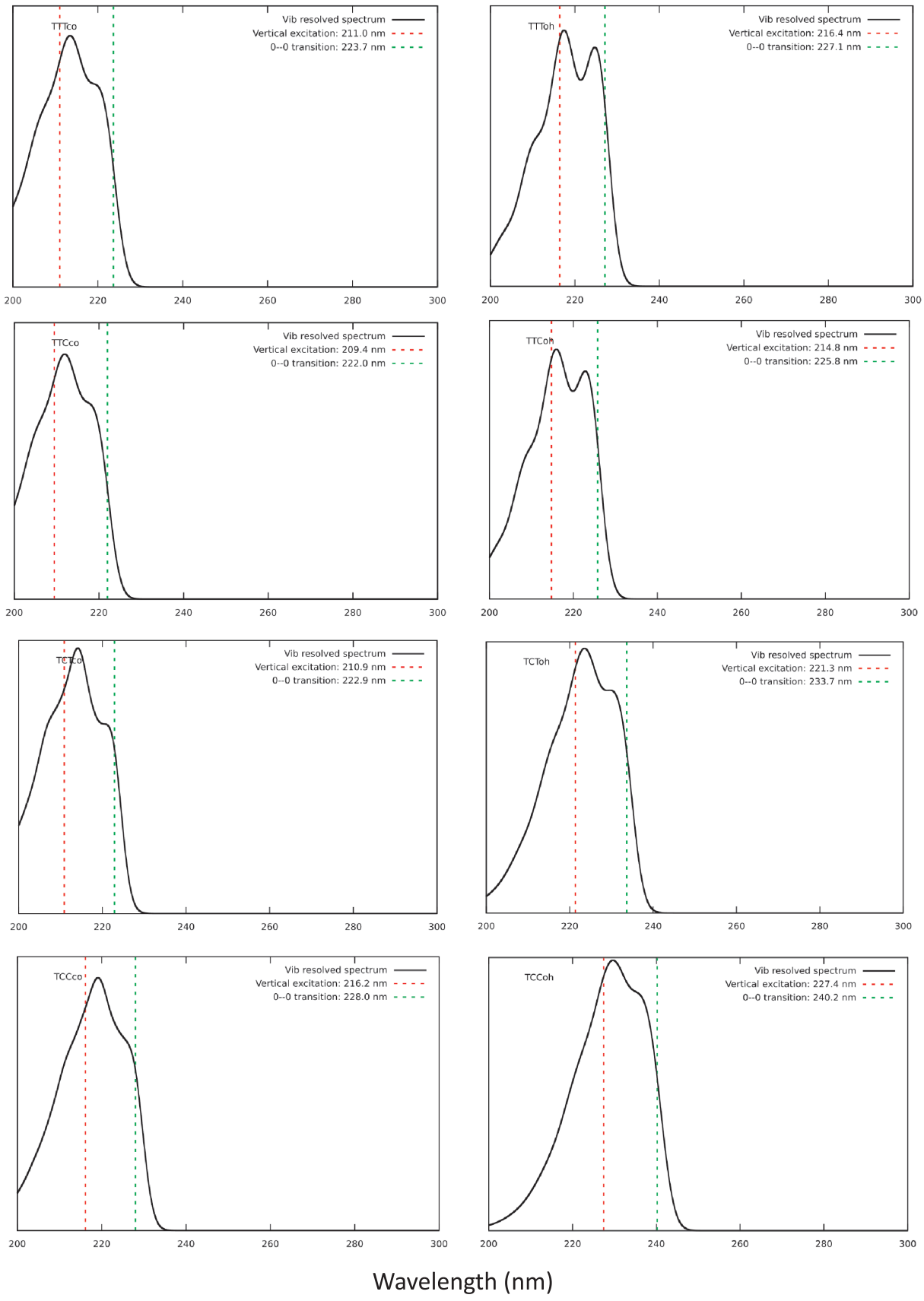

Figure S5: Theoretical UV absorption spectra of TXXxx species (for calculation details, see text)